Enzyme level N and O isotope effects of assimilatory and dissimilatory nitrate reduction

Lija A. Treibergs,[a] Julie Granger*
Department of Marine Sciences, University of Connecticut, Groton, Connecticut

Abstract

To provide mechanistic constraints to interpret nitrogen (N) and oxygen (O) isotope ratios of nitrate (NO_3^-), $^{15}N/^{14}N$ and $^{18}O/^{16}O$, in the environment, we measured the enzymatic NO_3^- N and O isotope effects ($^{15}\varepsilon$ and $^{18}\varepsilon$) during its reduction by NO_3^- reductase enzymes, including (1) a prokaryotic respiratory NO_3^- reductase, *Nar*, from the heterotrophic denitrifier *Paracoccus denitrificans*, (2) eukaryotic assimilatory NO_3^- reductases, *eukNR*, from *Pichia angusta* and from *Arabidopsis thaliana*, and (3) a prokaryotic periplasmic NO_3^- reductase, *Nap*, from the photoheterotroph *Rhodobacter sphaeroides*. Enzymatic *Nar* and *eukNR* assays with artificial viologen electron donors yielded identical $^{18}\varepsilon$ and $^{15}\varepsilon$ of $\sim$28‰, regardless of $[NO_3^-]$ or assay temperature, suggesting analogous kinetic mechanisms with viologen reductants. *Nar* assays fuelled with the physiological reductant hydroquinone (HQ) also yielded $^{18}\varepsilon \approx {}^{15}\varepsilon$, but variable amplitudes from 21‰ to 33.0‰ in association with $[NO_3^-]$, suggesting analogous substrate sensitivity in vivo. *Nap* assays fuelled by viologen revealed $^{18}\varepsilon$:$^{15}\varepsilon$ of 0.50, where $^{18}\varepsilon \approx 19$‰ and $^{15}\varepsilon \approx 38$‰, indicating a distinct catalytic mechanism than *Nar* and *eukNR*. *Nap* isotope effects measured in vivo showed a similar $^{18}\varepsilon$:$^{15}\varepsilon$ of 0.57, but reduced $^{18}\varepsilon \approx 11$‰ and $^{15}\varepsilon \approx 19$‰. Together, the results confirm identical enzymatic $^{18}\varepsilon$ and $^{15}\varepsilon$ during NO_3^- assimilation and denitrification, reinforcing the reliability of this benchmark to identify NO_3^- consumption in the environment. However, the amplitude of enzymatic isotope effects is apt to vary in vivo. The distinctive signature of *Nap* is of interest for deciphering catalytic mechanisms but may be negligible in most environments given its physiological role.

Nitrogen (N) is an essential plant nutrient, whose availability has substantial influence on the productivity of terrestrial and marine ecosystems (reviewed by Gruber and Galloway 2008). It is thus important to understand the sources, sinks and cycling of bioavailable nitrogen on local, regional and global scales. To this end, the naturally occurring stable N and O (oxygen) isotope ratios of nitrate (NO_3^-; $^{15}N/^{14}N$ and $^{18}O/^{16}O$, respectively) provide a useful tracer to investigate N cycling in the environment (reviewed by Kendall et al. 2007; Casciotti 2016). By convention, isotope ratios are reported using delta notation, where $\delta^{15}N = ([^{15}N/^{14}N]_{sample}/[^{15}N/^{14}N]_{air} - 1) \times 1000$ and $\delta^{18}O = ([^{18}O/^{16}O]_{sample}/[^{18}O/^{16}O]_{SMOW} - 1) \times 1000$, in units of per mille (‰). The $\delta^{15}N_{NO_3}$ and $\delta^{18}O_{NO_3}$ register the isotopic imprints of NO_3^- sources, as well as those imparted by

transformations to which it was subject. NO_3^- isotopes thus integrate the spatial and temporal variability inherent to N transformations in the environment, which is difficult to capture otherwise. Measured in tandem, the coupled $\delta^{15}N_{NO_3}$ and $\delta^{18}O_{NO_3}$ further provide complementary signatures of cooccurring N transformations that could not be disentangled from measurements of $\delta^{15}N_{NO_3}$ alone (reviewed by Casciotti 2016).

The two major biological NO_3^- consumption pathways in the N cycle are NO_3^- assimilation and denitrification. Denitrification refers to the microbially mediated respiratory reduction of NO_3^- to N_2 gas. Both of these reactions impart N and O isotopic enrichments to the unconsumed NO_3^- pool. During assimilation and denitrification, NO_3^- containing the light isotopes, ^{14}N and ^{16}O, reacts faster than heavy isotopologues, leading to a progressive enrichment of both ^{15}N and ^{18}O of the remaining NO_3^- pool as it is consumed (Granger et al. 2004, 2008). The degree of isotopic discrimination is quantified by the kinetic isotope effect, $\varepsilon = (^{light}k/^{heavy}k - 1) \times 1000$, expressed in per mille (‰), where the $^{light}k$ and $^{heavy}k$ are the respective reaction rate coefficients for the light and the heavy isotope-bearing molecules (Mariotti et al. 1981).

Culture studies of NO_3^- consumption by phytoplankton and by denitrifying bacteria have revealed that N and O isotope discrimination of the heavy isotopologues of NO_3^- occurs intracellularly during enzymatic bond breakage by the respective assimilatory and respiratory NO_3^- reductases (Shearer et al. 1991; Needoba et al. 2004; Granger et al. 2004, 2008; Karsh et al. 2014). The isotopic enrichment of internal NO_3^- propagates to the external medium due to passive cellular efflux, given a favorable electrochemical gradient. The magnitude of the organism-level N and O isotope effects recorded in the external medium ($^{15}\varepsilon_{organism}$ and $^{18}\varepsilon_{organism}$) thus reflect the fraction of NO_3^- effluxed out of the cell relative to cellular NO_3^- uptake, where $\varepsilon_{organism}$ = efflux/uptake $\times \varepsilon_{enzyme}$ (Shearer et al. 1991; Needoba et al. 2004; Granger et al. 2004, 2008; Karsh et al. 2014). A peculiar characteristic of both assimilatory and respiratory NO_3^- isotope dynamics is that the O-to-N enrichments observed in NO_3^- covary equivalently ($\Delta\delta^{18}O{:}\Delta\delta^{15}N = 1$), such that $^{15}\varepsilon_{organism} = {}^{18}\varepsilon_{organism}$, regardless of growth conditions or isotope effect amplitudes (Granger et al. 2004, 2008, 2010; Kritee et al. 2012; Wunderlich et al. 2012). This coupling reflects that imparted internally by NO_3^- reductase (Granger et al. 2004, 2008; Karsh et al. 2014), as confirmed by in vitro enzymatic assays of the eukaryotic assimilatory NO_3^- reductase (*eukNR*) from the fungus *Aspergillus* sp. and from the diatom *Thalassiosira weissflogii* (Karsh et al. 2012). The *eukNR* assays also revealed invariant enzymatic isotope effects amplitudes, $^{15}\varepsilon_{eukNR}$ coupled to $^{18}\varepsilon_{eukNR}$, of $\sim27\permil$ for both of the experimental NO_3^- reductases (Karsh et al. 2012). The enzymatic N and O isotope effects are thus coherently higher than the upper end of the observed assimilatory N and O isotope effects ($\varepsilon_{eukNR} > \varepsilon_{organism}$), which range from $0\permil$ to $20\permil$ in culture cultures of eukaryotic phytoplankton (Wada and Hattori 1978; Montoya and McCarthy 1995; Waser et al. 1998; Needoba et al. 2003; Granger et al. 2004), and from $5\permil$ to $10\permil$ at the surface ocean (Wu et al. 1997; Sigman et al. 1999; Waser et al. 1999; Altabet 2001; Karsh et al. 2003; DiFiore et al. 2006).

The amplitude of the enzymatic isotope effects of *Nar*, the bacterial respiratory NO_3^- reductase, has not been verified directly in vitro, nor has its O-to-N coupling. The organism-level isotope effects for denitrification (henceforth referred to as $^{15}\varepsilon_{denit}$) observed in cultures and in the environment cover a broader range than observed for NO_3^- assimilation, from $2\permil$ to $30\permil$ (Wellman et al. 1968; Brandes et al. 1998; Barford et al. 1999; Voss et al. 2001; Granger et al. 2008; Kritee et al. 2012). This suggests that the enzymatic isotope effects, $^{15}\varepsilon_{Nar}$ (coupled to $^{18}\varepsilon_{Nar}$), may be upwards of $30\permil$, and that the ratio of cellular NO_3^- efflux to uptake may be much higher during denitrification than during NO_3^- assimilation (Granger et al. 2008; Kritee et al. 2012), given frequent observations of $^{15}\varepsilon_{denit} \geq 25\permil$ (e.g., Wellman et al. 1968; Barford et al. 1999; Granger et al. 2008).

Identifying the controls on the magnitude of the isotope effects for denitrification, $^{15}\varepsilon_{denit}$, has implications, among others, for constraining source and sink terms of reactive N to the global ocean. In particular, NO_3^- isotope ratios and associated $^{15}\varepsilon_{denit}$ amplitudes provide a conserved metric from which to construct a mass balance of nitrogen sources and sink terms to the global ocean (Brandes and Devol 2002). Such exercises, however, generally diagnose a massive, yet improbable, imbalance in the modern oceanic N budget (Brandes and Devol 2002; Deutsch et al. 2004; Eugster and Gruber 2012; DeVries et al. 2013), calling into question the validity of current estimates of the denitrification $^{15}\varepsilon_{denit}$ in the ocean (Kritee et al. 2012). The $^{15}\varepsilon_{denit}$ amplitude in the denitrifying water column at western ocean margins is generally estimated to be on the order of $25\permil$ (Brandes et al. 1998; Voss et al. 2001). The variability of $^{15}\varepsilon_{denit}$ in cultures, however, and its potential correlation with the cellular reduction rates therein (Kritee et al. 2012), may portend of comparable mutability in the environment (Casciotti et al. 2013; Buchwald et al. 2015).

Characterizing the origin of the invariant $\Delta\delta^{18}O{:}\Delta\delta^{15}N$ coupling of NO_3^- during it reductive consumption is also crucial to the study of N isotopes in the environment. In marine denitrifying systems, $\Delta\delta^{18}O{:}\Delta\delta^{15}N$ trajectories *greater* than 1 have been observed in oxygen-deficient zones of Eastern Pacific and Indian Oceans, which are best explained by the isotopic signal of denitrification partially overprinted by NO_3^- production by nitrification (Sigman et al. 2005; Casciotti and McIlvin 2007; Casciotti et al. 2013; Gaye et al. 2013; Bourbonnais et al. 2015; Buchwald et al. 2015). In contrast, a $\Delta\delta^{18}O{:}\Delta\delta^{15}N$ coupling of ~0.6 is customarily associated with dissimilative NO_3^- attenuation in freshwater lakes and groundwater aquifers (Kendall et al. 2007). This characteristic signal has traditionally been interpreted as reflecting the unique isotopic imprint of denitrification (Amberger and Schmidt 1987; Böttcher et al. 1990; Aravena and Robertson 1998; Kendall et al. 2007). However, this clearly conflicts observations from marine systems and from culture and enzymatic studies. Workers who have acknowledge this discrepancy invoke fundamental differences in fractionation between marine and freshwater denitrifying systems, including mutability of the *Nar*-mediated $\Delta\delta^{18}O{:}\Delta\delta^{15}N$ trajectory (Knöller et al. 2011), or a substantial contribution of the auxiliary *Nap* NO_3^- reductase to bulk NO_3^- reduction in freshwater systems (Frey et al. 2014; Wenk et al. 2014a). Alternatively, the divergence in $\Delta\delta^{18}O{:}\Delta\delta^{15}N$ coupling in freshwater systems compared to culture observations may portend of biological NO_3^- production by nitrification and/or anammox imprinted on the isotopic signal of denitrification (Wunderlich et al. 2013; Wenk et al. 2014b; Granger and Wankel in unpubl.).

Finally, isotope fractionation associated with enzymatic reactions can provide information about an enzyme's kinetic mechanism. Karsh et al. (2012) observed that the enzymatic isotope effect of *eukNR* $^{15}\varepsilon_{eukNR}$ (couple to $^{18}\varepsilon_{eukNR}$) remained invariant regardless NO_3^- concentration. The insensitivity of

ε_{eukNR} to substrate concentrations is consistent with two potential catalytic mechanisms, in which NO_3^- either binds to the prereduced enzyme or in which NO_3^- is in rapid equilibrium with the oxidized enzyme (Karsh et al. 2012). The enzyme-level N and O isotope effects of sister enzymes *Nar* and *Nap* may similarly provide constraints on their respective catalytic mechanisms.

We investigated NO_3^- N and O isotope fractionation during its reduction by a prokaryotic respiratory *Nar*, a prokaryotic auxiliary *Nap*, as well as eukaryotic assimilatory *eukNAR* NO_3^- reductase enzyme from cell homogenates or from purified extracts, in order to (1) provide additional insights into physiological mechanisms of NO_3^- isotope fractionation during its reductive consumption, (2) further establish the O-to-N coupling as robust benchmark to interpret NO_3^- isotope distributions in the environment, and (3) investigate the kinetic mechanisms of *Nar* and *Nap* compared to that of *eukNR*. The results corroborate trends observed previously for other eukaryotic assimilatory NO_3^- reductases (Karsh et al. 2012), and provide direct observations of N and O isotope effects imparted by the respective prokaryotic dissimilatory *Nar* and *Nap* NO_3^- reductases. The observations further reveal that the amplitude of NO_3^- reductase enzymatic isotope effects is prone to vary under certain conditions, which have implications for understanding their catalytic mechanisms and the expression of enzymatic isotope effects in vivo.

Materials and methods

NO_3^- reductase assays

Enzymatic assays were conducted on (1) cell homogenates from the denitrifying bacterial strain *Paracoccus denitrificans* (American Type Culture Collection [ATCC] 19367) cultured under anaerobic vs. aerobic conditions to favor expression of *Nar* vs. *Nap* nitrate reductase, respectively (as *Nap* is expressed during aerobic growth of *P. denitrificans*, whereas *Nar* is expressed during anaerobic growth; Sears et al. 1997), (2) cell homogenates from the photoheterotrophic bacterial strain *Rhodobacter sphaeroides* (Deutsche Sammlung von Mikroorganismen 158) cultured aerobically, targeting the expression of *Nap*, specifically, as *R. sphaeroides* does not possess *Nar*, and (3) purified extracts of recombinant eukaryotic assimilatory NO_3^- reductases (*eukNR*) from the flowering plant *Arabidopsis thaliana* (AtNaR: EC 1.7.1.1) and from the yeast *Pichia angusta* (YNaR1: EC 1.7.1.2), both purchased from NECi (nitrate.com).

Preparation of P. denitrificans *cell concentrates*

P. denitrificans was cultured in medium containing 30 g L^{-1} Bactro™ tryptic soy broth supplemented with 300 μmol L^{-1} KNO_3, 1 mmol L^{-1} $NaNH_4$, and 100 μmol L^{-1} K_2HPO_4. NH_4^+ was added in excess of nutritional requirements in order to inhibit the expression of the bacterial assimilatory NO_3^- reductase, *Nas*, thus ensuring that NO_3^- was reduced by *Nar* and/or *Nap* exclusively (Bender and Friedrich 1990). Media were sterilized by autoclaving for 1 h. A

large culture was initiated in an acid-washed 2 liters Erlenmeyer flask and grown at room temperature while continuously purged with lab air. After 3 d, when cell density was maximal, the flask was sealed to cutoff the oxygen supply and allow for the inception of denitrification. After 14 h, the absence of NO_3^- and NO_2^- was verified, at which point cells were harvested by centrifugation for 20 min at $12,000 \times g$. The cell pellet was resuspended in a 100 μmol L^{-1} potassium phosphate buffer solution (pH 7.9) containing Halt™ Protease Inhibitor Cocktail (to minimize protein breakdown) and 100 μmol L^{-1} ethylenediaminetetraacetic acid (EDTA). The cell concentrate was immediately flash frozen in liquid nitrogen, and transferred to a $-80°$ freezer for long-term storage.

An additional culture of *P. denitrificans* was grown under aerobic conditions to favor the expression of *Nap* and the suppression of *Nar*. Media specifications and growth conditions were as above. The culture, however, was purged with air continuously until harvest, to inhibit the expression of *Nar* (Korner and Zumft 1989). Prior to harvest, the culture was kept on ice during transport to the centrifuge to minimize any expression of *Nar* when cells were not actively purged with air. Cells were concentrated by centrifugation for 20 min at $12,000 \times g$ at 4°C. Cell pellets were resuspended in buffered solution and flash frozen as above.

Preparation of R. sphaeroides *cell concentrates*

In order to provide cellular extracts for *Nap* reductase assays, the photo-heterotrophic bacterial strain *R. sphaeroides* was grown in a modified RCV medium (4 g L^{-1} $MgSO_4$, 1.5 g L^{-1} $CaCl_2$, 40 mL L^{-1} 1% [wt/vol] EDTA; Weaver et al. 1975) containing 4 g L^{-1} Bactro™ tryptic soy broth amended with 300 μM KNO_3 and 0.05 g L^{-1} $NaNH_4$. NH_4^+ was added in excess to inhibit the expression of the prokaryotic assimilatory nitrate reductase *Nas* and ensure that all NO_3^- was being reduced by *Nap*. After autoclaving, 1 mL L^{-1} of filter-sterilized Teknova T1001 trace-metal mix and 1 mL of filter-sterilized *f/2* vitamins were added to the medium (Guillard 1975). A large batch culture was initiated in an acid-washed 2-liter Erlenmeyer flask and grown at room temperature while continuously purged with lab air. Cells were harvested by centrifugation and resuspended in buffered solution as above.

R. sphaeroides cultures were also initiated in the above-described medium in order to monitor the evolution of NO_3^- isotopes in vivo in two experimental treatments. Two consecutive sets of experimental cultures were grown aerobically (without aeration), either directly on the bench top (still) or on a rotary shaker, to compare isotope effects between the two treatments and to further compare in vivo to in vitro NO_3^- isotope effects associated with *Nap*.

Commercial stocks of purified eukaryotic NO_3^- reductases (eukNR)

Freeze dried, commercially prepared purified eukaryotic nitrate reductase (*eukNR*) enzyme preparations from *A. thaliana* and *P. angusta* (1 enzyme unit = 1 μmol NO_3^-

reduced min^{-1} at 25°C) were reconstituted in 1 mL of the accompanying assay buffer solution (25 mmol L^{-1} KH$_2$PO$_4$ [pH 7.5], 25% glycerol [vol/vol] and 25 μmol L^{-1} EDTA).

Enzymatic assay preparations

Initial *Nar* assays were conducted with anaerobically cultured *P. denitrificans* cell suspensions taken directly from the frozen stock with no additional preparation (Table 1). In all subsequent cell suspension assays (*P. denitrificans* and *R. sphaeroides*), the frozen stock of cell suspension was thawed in ice water to minimize enzyme degradation, and working fractions were supplemented with 1% (vol/vol) Triton-X 100 and subjected to 2 freeze-thaw cycles in liquid nitrogen to further promote membrane breakdown and protein solubilization. *P. denitrificans* assays were conducted either at room temperature (~20°C) or in a cold room maintained at 4°C to assess potential temperature effects on the enzymatic isotope effect of dissimilatory nitrate reductases. Prior to performing these experiments, all reagents were pre-chilled to 4°C in the cold room. All *R. sphaeroides* and *eukNR* assays were conducted at room temperature.

Assays were conducted in 15-mL conical polypropylene centrifuge tubes. Assay preparations contained 0.5 mL or 1 mL of cell suspension or of purified *eukNR* in buffer solution, 0.2–2.5 mL of 200 μmol L^{-1} reducing agent—either membrane-permeant benzyl viologen dichloride (CAS: 1102-19-8; Sigma-Aldrich), methyl viologen dichloride hydrate (CAS: 75365-73-0; Sigma-Aldrich), or hydroquinone (HQ: for dissimilatory reductases only; CAS: 123-31-9; MP Organics)—0.2 mL or 1 mL of 10 mmol L^{-1} KNO$_3$ to a final concentration of 200 μmol L^{-1} or 1000 μmol L^{-1}, and the remaining volume of 100 mmol L^{-1} phosphate buffer (pH 7.9) containing 100 μmol L^{-1} to a final assay volume of 10 mL. After removing an initial 1 mL aliquot for the quantitation of initial [NO$_3^-$] and [NO$_2^-$] and δ^{15}N$_{NO_3}$, the reaction was commenced by the addition of 1 mL of 57 mmol L^{-1} sodium dithionite in 29 mmol L^{-1} sodium bicarbonate, which reduces the electron donor. Initial [NO$_3^-$] and [NO$_2^-$] values are corrected for this dilution. Sequential 1 mL samples were drawn approximately every 90 s during room temperature assays and every 3 min during assays conducted at 4°C. Samples were mixed vigorously on a vortex mixer for 30 s immediately upon collection to halt the reaction through oxidation of the methyl or benzyl viologen or HQ. In order to ensure complete cessation of enzyme activity, samples were placed in an 80°C water bath for 2–10 min. In selected assays, additional subsamples (~50 μL) were drawn throughout the assay reactions for determination of [NO$_2^-$], which was measured upon sample collection.

NO$_2^-$ was then removed from the assay sub-samples via the addition of 55 μL 4% (wt/vol) sulfamic acid in 10% (vol/vol) HCl (Granger and Sigman 2009). In two assays (Fig. S1 and Table 1), subsets of samples were also subject to an alternate NO$_2^-$ removal method using ascorbic acid under He

purging (Granger et al. 2006) to compare NO$_2^-$ removal effectiveness at elevated [NO$_2^-$] to [NO$_3^-$] ratios (Fig. S1 and Table 1). Following nitrite removal, samples were returned to neutral pH with the addition of dilute NaOH and frozen for short-term storage.

Determination of [NO$_2^-$] and [NO$_3^-$]

[NO$_2^-$] was measured in the 50 μL samples by chemiluminescence detection on a NO$_x$ analyzer (model T200 Teledyne Advanced Pollution Instrumentation) following reduction to nitric oxide (NO) in a heated iodine solution (Garside 1982). Following NO$_2^-$ removal, [NO$_3^-$] was similarly determined by chemiluminescence detection on the NO$_x$ analyzer following conversion to NO in a heated vanadium solution (Braman and Hendrix 1989).

Determination of NO$_3^-$ δ^{15}N and δ^{18}O

NO$_3^-$ δ^{15}N and δ^{18}O were determined with the denitrifier method (Sigman et al. 2001; Casciotti et al. 2002), wherein denitrifying bacteria lacking terminal nitrous oxide reductase (*P. chlororaphis* f. sp. *aureofaciens* ATCC 1398) quantitatively convert NO$_3^-$ in aqueous samples to N$_2$O gas, which is then extracted, purified, and analyzed through a modified Thermo-Scientific Gas Bench II and Delta V Advantage gas chromatograph isotope ratio mass spectrometer. Samples were standardized through comparison to reference standards IAEA-N3, USGS-34, and USGS-32, which have δ^{15}N (vs. air N$_2$) and δ^{18}O (vs. V-SMOW) of 4.7‰ and 25.6‰, −1.8‰ and −27.9‰, and 180‰ and 25.6‰, respectively (Gonfiantini et al. 1995; Böhlke et al. 2003) after individually being referenced to pure N$_2$O injections from a common reference gas cylinder. Samples were also corrected for a bacterial "blank" when present, defined as any N$_2$O produced by bacteria in the absence of sample injection.

Estimates of the N and O isotope effects ($^{15}\varepsilon$ and $^{18}\varepsilon$, respectively) were derived by fitting NO$_3^-$ δ^{15}N and δ^{18}O to the linear equations (Mariotti et al. 1981):

$$\ln\left(\delta^{15}N+1\right) = \ln\left(\delta^{15}N_{initial}+1\right)+{}^{15}\varepsilon\ln\left(NO_3^-\right) \quad (1a)$$

$$\ln\left(\delta^{18}O+1\right) = \ln\left(\delta^{15}O_{initial}+1\right)+{}^{18}\varepsilon\ln\left(NO_3^-\right) \quad (1b)$$

Error on respective slopes, corresponding to ε, was calculated using model II geometric mean regression analysis that factors error associated with individual measures on both the *x*- and *y*-coordinates (Sokal and Rohlf 1995; Peltzer 2007). Standard deviations for δ^{15}N and δ^{18}O were calculated from analytical replicates. Measurement errors for [NO$_3^-$] were assigned a 3% of the reported [NO$_3^-$], a representative estimate based on the mean precision of [NO$_3^-$] measured from standards of known concentrations. For graphical presentation, the isotope ratio measurements were plotted against the ln[NO$_3^-$] in a simplified version of the Rayleigh model in which the slope to the linear fit approximates $^{15}\varepsilon$ and $^{18}\varepsilon$ (e.g., $\delta^{15}N = \delta^{15}N_{initial} - {}^{15}\varepsilon \ln[NO_3^-]$; Mariotti et al. 1981).

Table 1. Estimates of NO_3^- N and O enzymatic isotope effects and the ratio of O and N isotopic fractionation ($\Delta\delta^{18}O{:}\Delta\delta^{15}N$) for NO_3^- reductase assays of cell homogenates of *P. denitrificans* and *R. sphaeroides*, and of purified *eukNR* extracts (AtNar and YNar).

Enzyme Prep	Culture	Cells lysed	Reductant	[Red] (μM)	$[NO_3^-]_{initial}$ (μM)	Assay T (˚C)	NO_2^- removal	$^{15}\varepsilon_{enzyme} \pm \sigma$ (‰)	$^{18}\varepsilon_{enzyme} \pm \sigma$ (‰)	$\Delta\delta^{18}O{:}\Delta\delta^{15}N\pm\sigma$	N
P. denitrificans	Anaerobic	No	BeVi	200	200	20	Sulfamic	6.6±0.8	6.4±0.7	0.97±0.02	8
P. denitrificans	Anaerobic	No	BeVi	200	200	20	Sulfamic	10.2±0.9	10.0±0.6	0.98±0.01	5
P. denitrificans	Anaerobic	No	BeVi	200	700	20	Sulfamic	8.9±0.3	9.0±0.4	1.01±0.01	5
P. denitrificans	Anaerobic	No	BeVi	200	1000	20	Sulfamic	8.4±0.8	8.7±0.5	1.03±0.01	5
P. denitrificans	Anaerobic	Yes	BeVi	200	200	20	Sulfamic	27.1±1.0	26.5±0.9	0.97±0.01	4
P. denitrificans	Anaerobic	Yes	BeVi	200	1000	20	Sulfamic	27.0±1.6	27.0±1.4	1.00±0.01	4
P. denitrificans	Anaerobic	Yes	BeVi	200	1000	20	Sulfamic	28.6±2.1	27.4±1.1	0.95±0.01	4
P. denitrificans	Anaerobic	Yes	MeVi	200	200	20	Sulfamic	27.1±0.9	26.5±0.9	0.97±0.01	4
P. denitrificans	Anaerobic	Yes	MeVi	200	1000	20	Sulfamic	28.9±1.0	26.6±0.9	0.92±0.01	4
P. denitrificans	Anaerobic	Yes	MeVi	200	1000	4	Sulfamic	28.7±1.2	27.6±1.9	0.97±0.01	5
P. denitrificans	Aerobic	Yes	MeVi	200	1000	20	Sulfamic	26.3±2.2	26.0±1.9	0.99±0.01	8
P. denitrificans	Aerobic	Yes	MeVi	200	1000	20	Sulfamic	28.2±1.6	27.4±1.6	1.00±0.01	11
P. denitrificans	Anaerobic	Yes	HQ	200	200	20	Sulfamic	21.8±3.6	21.4±3.1	0.98±0.01	3
P. denitrificans	Anaerobic	Yes	HQ	200	200	20	Sulfamic	28.6±1.1	26.9±0.5	0.92±0.03	3
P. denitrificans	Anaerobic	Yes	HQ	200	200	20	Sulfamic	22.9±1.5	24.0±1.5	1.04±0.01	4
P. denitrificans	Anaerobic	Yes	HQ	200	200	20	Sulfamic	25.8±3.3	26.4±3.4	1.02±0.01	4
P. denitrificans	Anaerobic	Yes	HQ	200	200	20	Ascorbate	21.7±1.9	19.9±1.7	0.90±0.01	10
P. denitrificans	Anaerobic	Yes	HQ	200	1000	20	Sulfamic	33.0±4.3	31.8±4.1	0.96±0.01	3
P. denitrificans	Anaerobic	Yes	HQ	200	1000	20	Sulfamic	31.5±2.9	29.7±2.7	0.93±0.01	5
P. denitrificans	Anaerobic	Yes	HQ	500	1000	20	Sulfamic	31.8±2.9	30.4±1.9	0.95±0.01	7
P. denitrificans	Anaerobic	Yes	HQ	50	1000	20	Sulfamic	30.8±0.3	29.6±0.4	0.95±0.01	7
P. denitrificans	Anaerobic	Yes	HQ	200	1000	20	Sulfamic	27.5±1.5	26.4±1.4	0.96±0.01	11
P. denitrificans	Anaerobic	Yes	HQ	200	1000	20	Sulfamic	26.5±1.0	26.0±0.9	0.98±0.01	10
P. denitrificans	Anaerobic	Yes	HQ	200	1000	20	Sulfamic	29.6±1.2	28.4±1.2	0.95±0.01	13
P. denitrificans	Anaerobic	Yes	HQ	200	1000	20	Sulfamic	28.4±1.2	27.9±1.2	0.99±0.01	12
P. denitrificans	Aerobic	Yes	HQ	200	1000	20	Sulfamic	30.2±3.6	28.3±3.9	0.95±0.01	12
P. denitrificans	Anaerobic	Yes	HQ	200	1000	4	Sulfamic	26.1±1.3	24.5±1.4	0.91±0.10	6
P. denitrificans	Anaerobic	Yes	HQ	200	1000	4	Sulfamic	26.3±1.4	25.9±1.4	0.98±0.01	8
P. denitrificans	Anaerobic	Yes	HQ	200	1000	4	Sulfamic	27.3±2.3	26.6±2.2	0.98±0.01	6
P. denitrificans	Anaerobic	Yes	HQ	200	1000	4	Ascorbate	27.9±0.7	26.7±0.8	0.95±0.01	9
R. sphaeroides	Aerobic	Yes	MeVi	200	300	20	Sulfamic	37.4±3.9	18.7±1.9	0.50±0.01	10
R. sphaeroides	Aerobic	Yes	MeVi	200	300	20	Sulfamic	39.8±4.8	19.9±2.4	0.49±0.01	8
AtNar	-	-	MeVi	200	400	20	Sulfamic	25.6±1.5	25.5±1.1	0.99±0.01	13
YNar	-	-	MeVi	200	900	20	Sulfamic	28.0±2.5	27.5±2.3	0.94±0.01	12
YNar	-	-	MeVi	200	400	20	Sulfamic	27.2±2.3	25.0±2.0	0.93±0.01	10

Results

$[NO_3^-]$ decreased with time in all nitrate reductase assays (Fig. S2a). In assays where $[NO_2^-]$ was measured concurrently, it accumulated to a concentration equivalent of the coincident NO_3^- drawdown (Fig. S3). Dissimilatory *Nar* NO_3^- reductase assays with benzyl or methyl viologen generally had faster initial reaction rates than corresponding assays with HQ at a given cell concentration (Fig. S2b). For a given reductant, initial reaction rates were faster at higher initial NO_3^- concentrations, though not consistently so, and catalytic rates were faster for assays conducted at room temperate (20°C) compared to 4°C (data not shown).

As $[NO_3^-]$ decreased, the $\delta^{15}N$ and $\delta^{18}O$ of the residual NO_3^- pool increased concomitantly. NO_2^- removal with sulfamic acid was only effective to a point around 1:25 to 1:50 $[NO_3^-]{:}[NO_2^-]$, in keeping with the limitations of the method (Granger and Sigman 2009), evidenced by a tendency for observed $[NO_3^-]$ to plateau at low relative concentrations (around 20–40 μM) in association with haphazard O vs. N isotope ratios (Fig. S1). Two assays in which NO_2^- in subsamples was removed with ascorbic acid (Granger et al. 2006) in lieu of sulfamic acid confirmed a complete NO_3^- drawdown and coherent Rayleigh distillation at lower $[NO_3^-]$, contrasting corresponding assay sub-samples treated
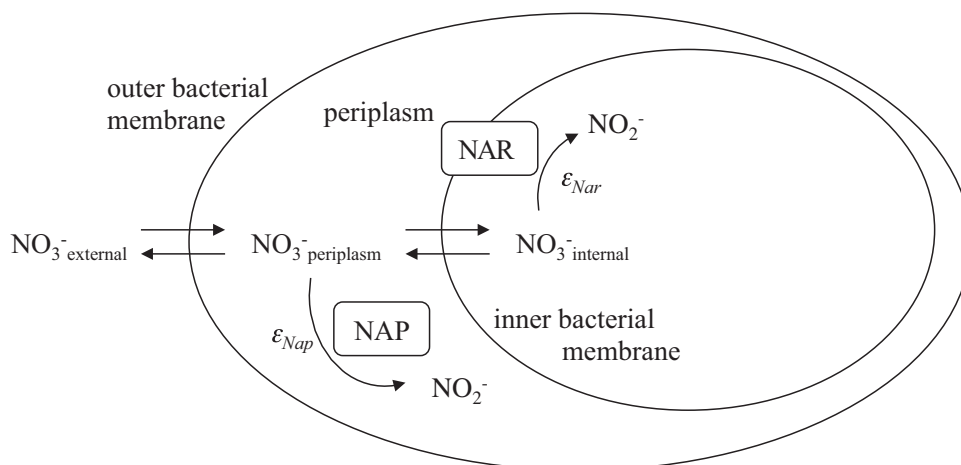
Fig. 1. Schematic of NO_3^- N and O isotope fractionation by the bacterial respiratory *Nar* and auxiliary *Nap* NO_3^- reductases of denitrifiers such as *P. denitrificans*. NO_3^- diffuses into the periplasm where it can be reduced to NO_2^- by *Nap*, which is expressed during aerobic growth and/or during transition to anaerobeosis. Assuming complete equilibration of external and periplasmic NO_3^- pools, the enzymatic N and O isotope effects of *Nap* are expressed fully in external NO_3^-. During anaerobic growth, NO_3^- is transported actively across the cell membrane, where it is reduced to NO_2^- by the membrane-bound respiratory *Nar*. The enzymatic N and O isotope effects imparted on internal NO_3^- by *Nar* are propagated to the external medium as unconsumed NO_3^- effluxes out of the cell, given a favorable electrochemical gradient across the cytoplasmic membrane. The enzymatic N and O isotope effects of *Nar* are thus expressed partially in external NO_3^-, as a function of cellular NO_3^- uptake to efflux.
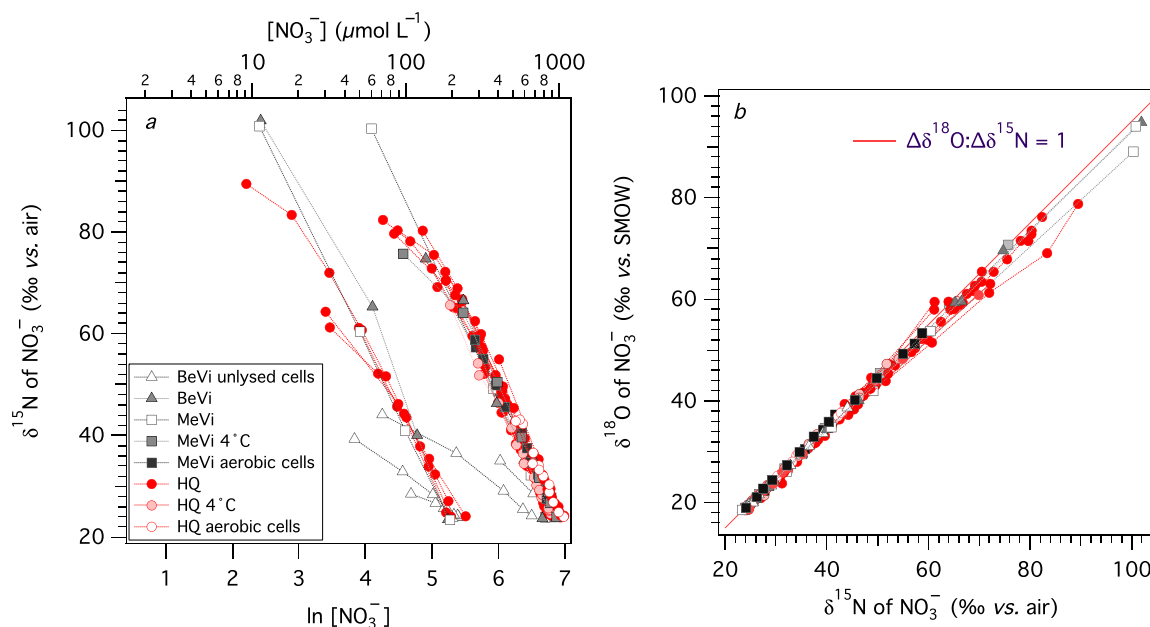

Fig. 2. (**a**) NO_3^- δ^{15}N vs. $\ln[NO_3^-]$ for enzymatic NO_3^- reduction assays by *P. denitrificans* cell homogenates. Assays were conducted with homogenates from anaerobic vs. aerobic cultures, of unlysed vs. lysed cells, with benzyl viologen, methyl viologen, or hydroquionone, at 1 mmol L^{-1} vs. 200 μmol L^{-1} initial $[NO_3^-]$, and at room temperature vs. 4°C. The slope of the linear regression for each assay approximates the N isotope effect, $^{15}\varepsilon_{enzyme}$. (**b**) NO_3^- δ^{18}O plotted against the corresponding δ^{15}N for *P. denitrificans* NO_3^- reductase assays. A line with a slope of 1 is shown for reference.

with sulfamic acid (Fig. S1 and Table 1). Thus, estimates of isotope effects describe the Rayleigh trend minus points in which δ^{15}N and δ^{18}O were decoupled and incoherent.

Among all *P. denitrificans* assays (anaerobic or aerobic cell suspensions), the progressive increase in δ^{15}N with decreasing $[NO_3^-]$ was similar to the corresponding δ^{18}O increase, regardless of reductant type, initial $[NO_3^-]$, assay temperature, and whether cell suspensions were fully lysed (Table 1 and Fig. 2a). The relative change in δ^{18}O ($\Delta\delta^{18}$O $= \delta^{18}$O $- \delta^{18}$O$_{initial}$) vs. that in δ^{15}N ($\Delta\delta^{15}$N $= \delta^{15}$N $- \delta^{15}$N$_{initial}$), hereafter referred to

as $\Delta\delta^{18}O{:}\Delta\delta^{15}N$, averaged $0.97 \pm 0.01(\sigma)$ among *P. denitrificans* assays. The O-to-N coupling persisted regardless of curvature in Rayleigh space, observed predominantly in assays fuelled by HQ.
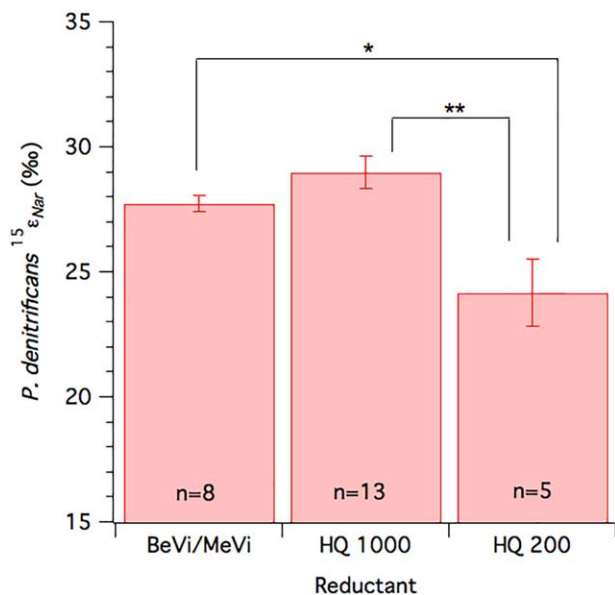

Fig. 3. Mean $^{15}\varepsilon_{enzyme}$ observed for viologen-fuelled (BeVi/MeVi) assays of anaerobic *P. denitrificans* homogenates, compared to HQ-fuelled assays at 1000 μmol L^{-1} and 200 μmol L^{-1} initial [NO$_3^-$]. The mean $^{15}\varepsilon_{enzyme}$ among HQ 200 assays differed significantly from that of both HQ 1000 assays (**$p \leq 0.01$) and BeVi/MeVi assays (*$p \leq 0.05$).

The magnitude of the $^{15}\varepsilon_{enzyme}$ (and coupled $^{18}\varepsilon_{enzyme}$) determined by Rayleigh linearization differed among *P. denitrificans Nar* assays fuelled by viologen reductants, from 6.6‰ to 28.9‰ (Table 1 and Fig. 2a). The lowest values on the order of 6‰ – 9‰ were observed only in initial assays with unlysed cell suspensions fuelled by benzyl viologen. Subsequent assays with lysed cell suspensions fuelled by either benzyl or methyl viologen yielded a narrow range of isotope effects averaging $27.9 \pm 0.9(\sigma)$‰ among assays ($n = 6$ assays), irrespective of initial [NO$_3^-$] or of assay temperature. Viologen-fuelled assays of *P. denitrificans* cultured aerobically to favor the expression of *Nap* had $^{15}\varepsilon_{enzyme}$ of $27.2 \pm 1.3(\sigma)$‰ ($n = 1$ assay) similar to corresponding assays with anaerobic cell suspensions (Table 1 and Fig. 2). Among all viologen-fuelled assays, the $\delta^{15}N$ (and $\delta^{18}O$) change remained roughly linear with decreasing [NO$_3^-$], save for one assay conducted at 4°C, where $^{15}\varepsilon_{enzyme}$ (and $^{18}\varepsilon_{enzyme}$) appeared to decrease at lower [NO$_3^-$].

Assays of lysed *P. denitrificans* homogenate fuelled by HQ yielded a broader range of $^{15}\varepsilon_{enzyme}$ values (and $^{18}\varepsilon_{enzyme}$) in lysed cell suspensions from 21.7‰ to 33.0‰ (Table 1 and Fig. 2). Higher $^{15}\varepsilon_{enzyme}$ (and $^{18}\varepsilon_{enzyme}$) values were largely associated with higher initial [NO$_3^-$] of 1 mmol L^{-1}, averaging $29.0 \pm 2.3(\sigma)$‰ among assays ($n = 13$ assays). Lower $^{15}\varepsilon_{enzyme}$ (and $^{18}\varepsilon_{enzyme}$) values largely corresponded to assays with 200 μmol L^{-1} initial [NO$_3^-$], averaging $24.2 \pm 3.0(\sigma)$‰ among assays ($n = 5$). An ANOVA signaled significant differences in $^{15}\varepsilon_{enzyme}$ means among three assay groups ($F(2,22) = 8.99$, $p = 0.001$): a Tukey post hoc test specified that the lower $^{15}\varepsilon_{enzyme}$ values at HQ-fuelled assays with low
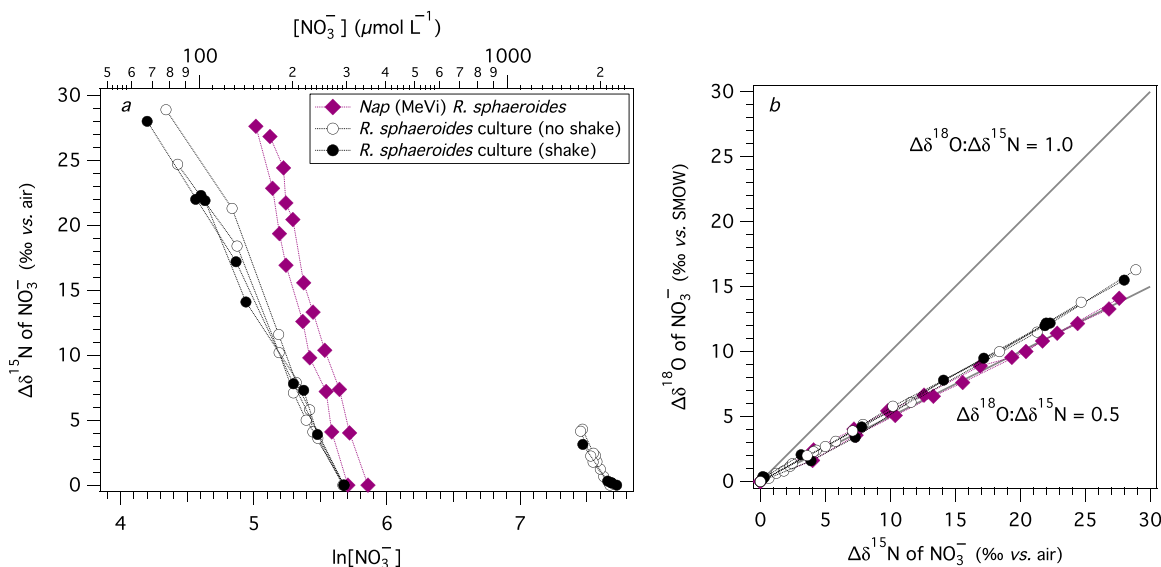

Fig. 4. (**a**) NO$_3^-$ $\delta^{15}N$ vs. ln[NO$_3^-$] for growing cultures of *R. sphaeroides* and for assays of enzymatic NO$_3^-$ reduction by *R, sphaeroides* cell homogenates. Two sets of cultures were initiated at 400 μmol L^{-1} vs. 2 mmol L^{-1} initial [NO$_3^-$], respectively, and grown on the bench-top or on a shaker. Enzymatic assays were conducted at 250 μmol L^{-1} initial [NO$_3^-$] and fuelled by methyl viologen. (**b**) NO$_3^-$ $\delta^{18}O$ plotted against the corresponding $\delta^{15}N$ for cultures of *R. sphaeroides* and for assays of enzymatic NO$_3^-$ reduction by *R. sphaeroides* cell homogenates. Respective slopes of 1 and 0.5 are shown for reference.

Table 2. NO_3^- N and O isotope effects and the ratio of O-to-N fractionation ($\Delta\delta^{18}O{:}\Delta\delta^{15}N$) during aerobic growth of *R. sphaeroides* in still cultures *vs.* cultures on a shaker.

Experiment	Culture	$[NO_3^-]_{initial}$ (μM)	$^{15}\varepsilon_{organism} \pm \sigma$ (‰)	$^{18}\varepsilon_{organism} \pm \sigma$ (‰)	$\Delta\delta^{18}O : \Delta\delta^{15}N \pm \sigma$	N
1	No shake	2000	23.0 ± 2.1	13.6 ± 2.3	0.59 ± 0.03	6
1	No shake	2000	18.4 ± 2.8	10.3 ± 2.4	0.56 ± 0.03	4
1	Shake	2000	13.1 ± 3.9	8.3 ± 3.7	0.62 ± 0.04	5
2	No shake	300	22.6 ± 2.2	12.7 ± 2.3	0.56 ± 0.01	7
2	No shake	300	20.9 ± 1.8	11.6 ± 2.0	0.56 ± 0.01	7
2	Shake	300	19.0 ± 2.0	10.6 ± 2.5	0.55 ± 0.01	4
2	Shake	300	20.1 ± 1.7	11.4 ± 2.2	0.57 ± 0.01	7
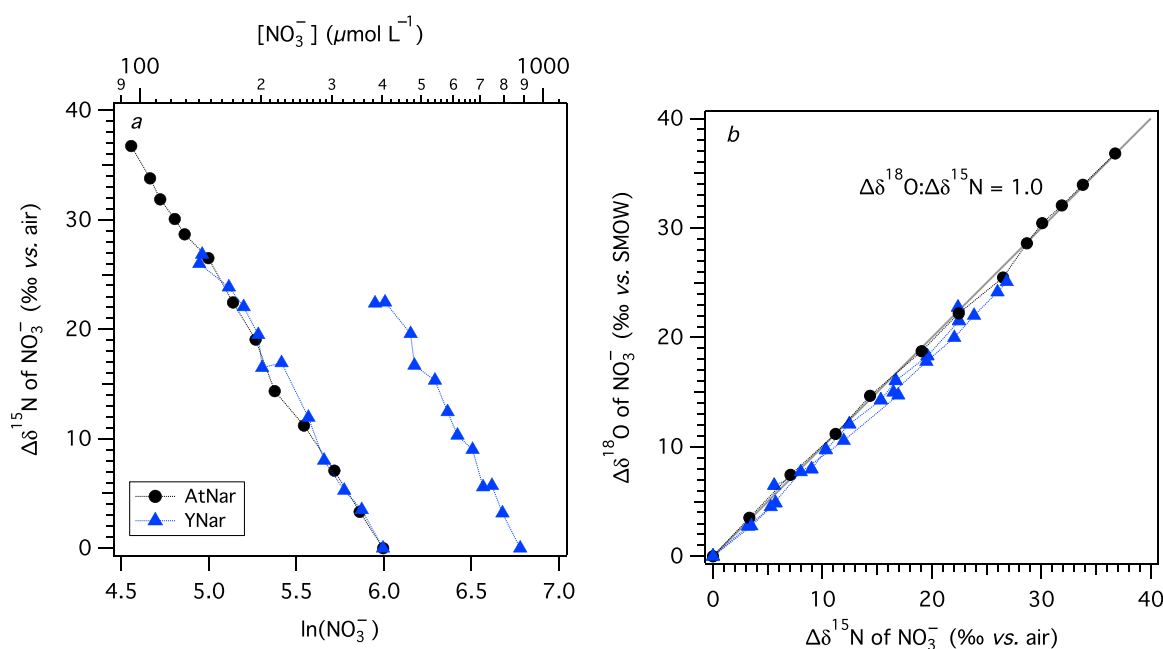
Fig. 5. (**a**) NO_3^- $\delta^{15}N$ vs. $\ln[NO_3^-]$ for purified recombinant eukaryotic NO_3^- reductases of *A. thaliana* (AtNar) and *P. angustus* (YNar). Assays were initiated at 400 μmol L^{-1} (AtNar and YNar) and 900 μmol L^{-1} NO_3^- (YNar) and fuelled with methyl viologen. (**b**) NO_3^- $\delta^{18}O$ plotted against the corresponding $\delta^{15}N$ for AtNar and YNar enzymatic assays. A slope of 1 is plotted for reference.

initial $[NO_3^-]$ differed significantly from $^{15}\varepsilon_{enzyme}$ in HQ-fuelled assays with high initial $[NO_3^-]$ ($p \leq 0.01$), and from $^{15}\varepsilon_{enzyme}$ in viologen-fuelled assays with both low and high $[NO_3^-]$ ($p \leq 0.05$), suggesting a sensitivity of $^{15}\varepsilon_{enzyme}$ (and $^{18}\varepsilon_{enzyme}$) to $[NO_3^-]$ specific to HQ assays (Fig. 3). The $^{15}\varepsilon_{enzyme}$ values of HQ-fuelled assays at high $[NO_3^-]$, however, did not differ significantly from viologen-fuelled assays. All assays fuelled by HQ showed evidence of a progressive decrease of $^{15}\varepsilon_{enzyme}$ (and $^{18}\varepsilon_{enzyme}$) as $[NO_3^-]$ decreased during the reactions (Fig. 2a), further suggesting a sensitivity of isotope effects to NO_3^- concentrations in HQ assays.

Enzymatic NO_3^- reductase assays conducted with cell suspensions of *R. sphaeroides* revealed more elevated $^{15}\varepsilon_{enzyme}$, averaging 37.4 ± 3.9($\sigma$)‰ in two assays, with a

corresponding $^{18}\varepsilon_{enzyme}$ of 18.7 ± 1.9(σ)‰, resulting in a $\Delta\delta^{18}O{:}\Delta\delta^{15}N$ of 0.50 ± 0.01 (Table 1 and Fig. 4). Isotope effects did not appear to decrease with $[NO_3^-]$, which reached 150 μmol L^{-1}. The isotope effects in growing cultures of *R. sphaeroides* were substantially lower than in corresponding enzymatic assays, averaging 19.6 ± 3.3(σ)‰ and 11.7 ± 1.7(σ)‰ for $^{15}\varepsilon_{enzyme}$ and $^{18}\varepsilon_{enzyme}$ (n = 7 assays) respectively, corresponding to a mean $\Delta\delta^{18}O{:}\Delta\delta^{15}N$ ratio of 0.57 ± 0.03 (Table 2 and Fig. 4). In the two growth experiments, cultures that were still vs. placed on a shaker during growth did not show systematic differences in N and O isotope effects. Isotope effects of the growing cultures appeared to decrease progressively at NO_3^- concentrations ≤ 120 μmol L^{-1}.

Assays conducted with commercial stocks of purified *eukNR* from *A. thaliana* (AtNar) and *P. angusta* (yeast-YNar) fuelled by MeV at 400 μmol L^{-1} initial [NO$_3^-$] yielded N isotope effects 25.6 ± 1.1(σ)‰ (n = 1 assay) and 27.6 ± 0.6(σ)‰ (n = 2 assays), respectively (Table 1 and Fig. 5). The $\Delta\delta^{18}$O:$\Delta\delta^{15}$N was ~1 for both enzymes, 0.99 ± 0.01 and 0.94 ± 0.01 for AtNar and YNar, respectively.

Discussion

Near equivalent N *vs.* O isotope fractionation by *Nar*

The O-to-N isotope coupling among all nitrate reductase assays of *P. denitrificans* cultured anaerobically was consistently on the order of ~1, regardless of reductant type, initial NO$_3^-$ concentration, or assay temperature. This confirms that *Nar*, the bacterial respiratory nitrate reductase, fractionates the heavy N and O isotopologues of NO$_3^-$ equivalently. This isotopic signal is consistent with those typically observed in pure cultures of denitrifiers (Granger et al. 2008; Kritee et al. 2012; Wunderlich et al. 2012), corroborating unequivocally that bond breakage by the *Nar* nitrate reductase enzyme is the dominant fractionating step during respiratory denitrification. The distinctive $\Delta\delta^{18}$O:$\Delta\delta^{15}$N signature of 1 associated with respiratory denitrification provides a benchmark for environmental studies, whereby respiratory NO$_3^-$ consumption can be identified from NO$_3^-$ isotope distributions, and distinguished from co-occurring N transformations. Our data further challenge the notion that the O-N coupling of denitrification is variable (Knöller et al. 2011). By itself, the invariant coupling of unity thus fails to explain the $\Delta\delta^{18}$O:$\Delta\delta^{15}$N ratio of 0.5 to 0.7 observed in association with N loss in groundwater aquifers and lakes. The coupling below 1 may be indicative of NO$_3^-$ production therein, by nitrification or anammox, co-incident with denitrification, thus overprinting the $\Delta\delta^{18}$O:$\Delta\delta^{15}$N of 1 (Granger and Wankel in review).

Variable amplitude of the enzymatic N and O isotope effects of *Nar*

The magnitude of the coupled N and O isotope effects varied among *P. denitrificans Nar* assays. Lower $^{15}\varepsilon$ (and $^{18}\varepsilon$) values of 6‰ – 10‰ in unlysed cell suspensions likely reflected incomplete equilibration of intracellular vs. external NO$_3^-$ pools, thus dampening propagation of the *Nar*-mediated enzymatic isotope effect to the external buffer. The isotope effects observed among lysed cell suspensions, in contrast, ostensibly reflect the enzyme-level isotope effects, $^{15}\varepsilon_{Nar}$ and $^{18}\varepsilon_{Nar}$, unfettered by the influence of NO$_3^-$ uptake into and export from the cells – which can lower observed isotope effects (Fig. 1). Values of $^{15}\varepsilon_{Nar}$ (coupled to $^{18}\varepsilon_{Nar}$) in assays with lysed cell suspensions of *P. denitrificans* varied in association with the type reductant fuelling nitrate reductase activity. Viologen-fuelled assays yielded $^{15}\varepsilon_{Nar}$ and $^{18}\varepsilon_{Nar}$ values on the order of ~28‰, which were relatively invariant regardless of initial [NO$_3^-$] or assay temperature. The value of

28‰ is in the general range of maximum isotope effects observed for denitrification in cultures (Wellman et al. 1968, Barford et al. 1999; Granger et al. 2008) and in the environment (Brandes et al. 1998;. Voss et al. 2001). A recent study, however, reported a more elevated $^{15}\varepsilon$ for *Nar* purified from *Escherichia coli* of 31.6‰ using benzyl viologen as a reductant (Carlisle et al. 2014). This estimate, however, derived from a 2-point regression on the δ^{15}N of the NO$_2^-$ product and is thus subject to considerable uncertainty. Nevertheless, there *are* reports of higher denitrification isotope effects in vivo (Kritee et al. 2012), including some observation of a $^{15}\varepsilon_{denit}$ upwards of 31‰ for *P. denitrificans* grown in our laboratory (Dabundo 2014).

Elevated $^{15}\varepsilon_{Nar}$ (coupled to $^{18}\varepsilon_{Nar}$) values observed in some HQ-fuelled *Nar* assays, as high as 33‰, are consistent with reports of equally elevated isotope effects in cultures. The higher ε_{Nar} values were associated with high initial NO$_3^-$, whereas lower ε_{Nar} values generally occurred at lower initial NO$_3^-$, revealing a sensitivity of ε_{Nar} to [NO$_3^-$], specifically in HQ-fuelled assays. Moreover, in all HQ assays, ε_{Nar} decreased progressively at lower relative [NO$_3^-$]—regardless of initial [NO$_3^-$]—further revealing an influence of ambient [NO$_3^-$] on ε_{Nar} amplitudes.

The apparent sensitivity of ε_{Nar} to [NO$_3^-$] in the HQ-fuelled assays suggests that ε_{Nar} is likely variable in vivo. Interpretation of NO$_3^-$ isotope dynamics of denitrifiers thus far has rested on the assumption that ε_{Nar} is invariant in vivo, such that ε_{denit} is modulated exclusively by the ratio of cellular NO$_3^-$ uptake and efflux (Granger et al. 2004; Wunderlich et al. 2012; Kritee et al. 2012; Karsh et al. 2014). The current observations uncover additional complexity inherent to the expression of the organism-level denitrification isotope effects, which are likely sensitive to intracellular [NO$_3^-$] in addition to the ratio of uptake and efflux. Therefore, predictive or diagnostic constraints of the denitrification isotope effects necessitate a better understanding of cellular biochemistry and energetics in relation to environmental conditions.

Mechanistic basis of ε_{Nar} variability during catalysis

Analogous sensitivity of enzymatic isotope effects to substrate concentrations has been documented for *Nir*, the respiratory NO$_2^-$ reductase of denitrifiers (Bryan et al. 1983), which showed lowered N isotope effects in vitro at lower NO$_2^-$ concentrations vs. higher isotope effects at lower reductant concentrations. The authors argued that catalytic rates of NO$_2^-$ reductase, mediated by substrate and reductant concentrations, influence the expression of the intrinsic enzymatic isotope effect, $\varepsilon_{intrinsic}$, associated specifically with bond breakage. As described therein, enzyme-mediated chemical reactions often involve multiple steps in addition to the chemical reaction itself, and the magnitude of the observed isotope effect for a unidirectional enzyme-mediated reaction depends on the degree to which the isotopically-sensitive step of catalysis is rate-limiting. In the case of *Nar*,
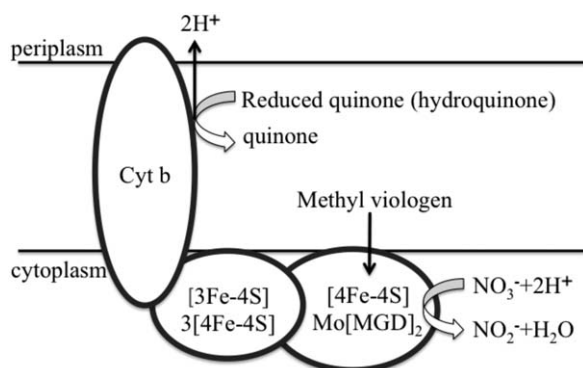
Fig. 6. Illustration of the subunit arrangement and cofactor content of the ubiquinol NO_3^- reductase (*Nar*) and the locations of electron transfer by reductants hydroquinone (in vivo reductant) and benzyl or methyl viologen (artificial reductant). Cyt *b* denotes the transmembrane b-type cytochrome subunit, and 3Fe-4S and 4Fe-4S indicate iron-sulfur clusters of varying forms within both the secondary and catalytic subunits. Mo[MGD]$_2$ denotes the molybdenum active site in the catalytic subunit. Figure reproduced from Berks et al. (1995).

NO_3^- reduction requires the succeeding reduction of three enzyme subunits as electrons are transferred from the quinol pool to the molybdenum active site of enzyme before the final reduction can take place. The speed of this electron transfer could affect the overall reaction rate of *Nar* and, and, consequently, the isotope effect. This is best explained by considering the irreversible enzymatic reaction, where

$$E + S \underset{k_{back}}{\overset{k_{forward}}{\rightleftarrows}} ES \xrightarrow{k_{catalysis}} EP \qquad (2)$$
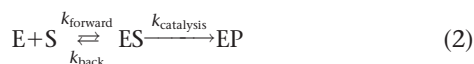
Once a substrate (S) binds with its enzyme (E) at a specific forward reaction rate, $k_{forward}$, to form an enzyme-substrate complex (ES), the substrate has one of two fates: it is either converted to product (P) by the enzyme at a specific catalytic rate, k_{cat}, or it is released from the enzyme at a specific back reaction rate k_{back}, rejoining the substrate pool. Theoretically, the observed isotope effect is then dependent on the relative reaction rates of catalysis and release (O'Leary 1980; Cook 1991).

$$\alpha_{enzyme} = \frac{\alpha_{intrinsic} + {k_{cat}}/{k_{back}}}{1 + {k_{cat}}/{k_{back}}} \qquad (3)$$

where $\alpha_{intrinsic}$ is the isotope effect associated specifically with the catalytic step, quantified as $\alpha_{intrinsic} = {}^{light}k_{cat}/{}^{heavy}k_{cat}$ (such that $\varepsilon_{intrinsic} [\text{‰}] = [\alpha_{intrinsic} - 1] \times 1000$). If all substrate that binds the enzyme is converted to product, the observed enzymatic isotope effect, α_{enzyme}, will be one, such that ε_{enzyme} (where $\varepsilon_{enzyme} = [\alpha_{enzyme} - 1] \times 1000$), will be zero, assuming no fractionation associated with binding; this occurs if the rate of catalysis (k_{cat}) is fast relative to the rate of unbinding (k_{back}), such that the 'commitment to

catalysis,' k_{cat}/k_{back}, is large, dampening the expression of the intrinsic enzymatic isotope effect, $\varepsilon_{intrinsic}$ (Eq. 3). At the other limit, when k_{back} is extremely fast relative to k_{cat}, the full intrinsic isotope effect $\varepsilon_{intrinsic}$ is expressed in the residual substrate.

In our experiments, k_{cat} for *Nar* was likely modulated by the reductant type. The viologen reductants donate electrons directly to the molybdenum active site (Campbell 2001), whereas HQ, which is the in vivo electron donor, donates to the cytochrome *b* subunit of *Nar*, requiring the electrons to sequentially reduce the Fe-sulfur clusters of the other two *Nar* subunits in turn before reaching the active site (Fig. 6). Thus, electron transfer to the active site of *Nar*, and consequently catalysis, is expected to be slower via HQ than viologen. In this respect, viologen-fuelled assays generally proceeded more rapidly than corresponding assays fuelled by HQ (Fig. S2).

By speeding up k_{cat} relative to k_{back}, viologen reductants likely increase the commitment to catalysis (Campbell 2001), which could lower the isotope effect observed in the residual NO_3^- pool in assays fuelled by viologen compared to HQ. Therefore, the rate of internal electron transfer intrinsic to reduction by HQ likely influences the overall enzymatic reaction rate of *Nar*, such that the isotopically sensitive step of N–O bond breakage is not exclusively rate-limiting in the enzymatic reaction. The observed tendency for some higher isotope effects in HQ assays compared to analogous assays with viologen at high initial [NO_3^-] appear to validate this premise, as a lower commitment to catalysis in HQ assays would engender a higher expression of the intrinsic enzymatic isotope effect, $\varepsilon_{intrinsic}$, which could be as high as 33‰, the highest observed ε_{Nar}. Admittedly, ε_{Nar} values were not consistently more elevated in HQ assays compared to viologen assays, suggesting potentially overlooked influences of experimental conditions on catalytic rates among assays. Importantly, the elevated isotope effects observed in some HQ assays are likely not the result of analytical error, because both the NO_3^- concentrations and the NO_3^- isotopic analyses were conducted across multiple days with internal standards behaving as expected. Also, the possibility of incomplete cell lysis does not explain the variability in HQ-fuelled isotope effects, as analogous variability would also have been manifest in MeVi-fuelled assays. Thus, higher isotope effects in some HQ assays at high initial [NO_3^-] portend of slower electron shuttling to the active site of the enzyme compared to corresponding viologen assays, decreasing the commitment to catalysis, thus increasing expression of intrinsic enzymatic isotope effect.

In turn, the lower observed ε_{Nar} values in HQ-fuelled assays at lower initial [NO_3^-], as well tendency for ε_{Nar} to decrease with [NO_3^-] among all HQ assays, support the notion that lower substrate concentrations render substrate binding partially rate-determining relative to the catalytic rate, thereby reducing the proportion of substrate unbinding

(k_{back}/k_{cat}) from the enzyme. An increased commitment to catalysis at low [NO_3^-] consequently manifests as a lowered expression the intrinsic enzymatic isotope effect, $\varepsilon_{intrinsic}$, resulting in ε_{Nar} as low as ∼21‰ in some HQ-fuelled assays.

Based on the above reasoning connecting the commitment to catalysis to the observed ε_{Nar}, temperature could also exert some influence on the magnitude of ε_{Nar}, given the temperature sensitivity of enzymatic rate reactions. We hypothesized that reducing temperature would slow k_{cat}, potentially leading to a more elevated k_{back}/k_{cat} and a concurrently elevated isotope effect. However, assays conducted at 4°C with either viologen or HQ reductants had comparable isotope effects to corresponding assays at room temperature. It is possible the decrease in temperature did not influence the catalytic rate sufficiently to generate an observable difference in ε_{Nar}, or that the lower temperature slowed k_{back} proportionally to k_{cat}, such that the commitment to catalysis remained roughly the same.

Although not explored here, the concentration of reductant (HQ) could also influence commitment to catalysis and consequent enzymatic isotope effects, as per the respiratory NO_2^- reductase *Nir* (Bryan et al. 1983). Lower reductant concentrations could decrease commitment to catalysis, thus increasing the enzymatic isotope effect, whereas saturating reductant concentrations would tend to increase commitment to catalysis and consequently decrease the enzymatic isotope effect. Thus, expression of the enzymatic isotope effect in vivo is likely sensitive to intracellular [NO_3^-] in relation to the cellular energetics that influence the redox state of the quinone pool at the cell membrane (Dabundo 2014).

The substrate sensitivity of ε_{Nar} suggests an enzymatic mechanism in which the rate of electron transfer is partially rate-determining. In this respect, electron transfer is cited to constitute a rate-determining step of catalysis by *eukaryotic* NO_3^- reductases (Skipper et al. 2001; Barbier and Campbell 2005) which may have analogous kinetic mechanisms to *Nar*. However, substrate sensitivity of ε_{Nar} was not observed among assays fuelled by methyl or benzyl viologen—save for a single assay at lower temperature. This result is puzzling, because substrate sensitivity of ε_{Nar} should be even more evident given the increase in k_{cat} promulgated by viologen compared to HQ. In this respect, Karsh et al. (2012) similarly documented an invariant isotope effect of ∼27‰ for NO_3^- reduction by *eukNR* of *Aspergillus* sp. and of the diatom *T. weissflogii* in enzymatic assays fuelled by methyl viologen at different initial [NO_3^-]. Nevertheless, the authors recognized a potential sensitivity to reductant type by way of its effect on k_{cat}, had assays also been conducted with the in vivo electron donors NADH and NAD(P)H. The authors further stipulated that if $\varepsilon_{NAD[P]H} \cong \varepsilon_{MeVi}$, then the rate of electron transfer does not influence the magnitude of the isotope effect, suggesting that (1) NO_3^- binds to a reduced molybdenum (IV) center that has already received electrons, such that the electron transfer rate does not influence the

catalytic rate or (2) NO_3^- binds to an oxidized Mo(VI) center, but the substrate is in a state of rapid equilibrium with the enzyme, such that the rate of dissociation, $k_{back} \gg k_{cat}$, the rate of catalysis. This leads to a commitment to catalysis approaching zero and thus an observed isotope effect equal to that of the intrinsic isotope effect for N-O bond rupture, $\varepsilon_{intrinsic}$, regardless of electron transfer rate. As such, $\varepsilon_{intrinsic}$ of *eukNR* could be on the order of 27‰. Conversely, if $\varepsilon_{NAD[P]H} > \varepsilon_{MeVi}$, this would indicate that (3) NO_3^- binds to an oxidized Mo(VI) center where changes in k_{cat} effected by reductant type modulate the commitment to catalysis and the consequent enzymatic isotope effect. Our results for *Nar* indicate that ε_{Nar-HQ} can be both larger or less than $\varepsilon_{Nar-MeVi}$ depending on [NO_3^-], suggesting that NO_3^- is binding an oxidized Mo(VI) center and that commitment to catalysis is influenced by both the rate of internal electron transfer and by the concentration of NO_3^-. Therefore, substrates do *not* appear to be in rapid equilibrium with the enzyme, and the intrinsic enzymatic isotope effect associated specifically with bond breakage, $\varepsilon_{intrinsic-Nar}$, is ≥33‰. We posit that *eukNR* may exhibit similar dynamics when fuelled by in vivo reductants. Nevertheless, the insensitivity of both ε_{Nar} (and ε_{eukNR}; Karsh et al. 2012) and [NO_3^-] in viologen-fuelled assays remains difficult to reconcile and portends of a different kinetic mechanism of the enzyme with viologen electron donors than with in vivo quinone reductants. Indeed, *Nar* has been shown to display two catalytically competent yet kinetically distinct forms that can be reversibly interconverted as a function of electrochemical potential and substrate concentration (Anderson et al. 2001; Elliott et al. 2004; Jepson et al. 2004).

N and O isotope effects of the periplasmic NO_3^- reductase, *Nap*

Assays of cell homogenates of *P. denitrificans* grown aerobically, intended to capture isotope effects associate with NO_3^- reduction by the periplasmic *Nap* NO_3^- reductase, yielded enzymatic isotope effects indistinguishable from those of corresponding *Nar* assays, namely, a $\Delta\delta^{18}O:\Delta\delta^{15}N$ ratio of ∼1 and enzymatic isotope effects ∼27‰ in viologen-fuelled assays (Table 1 and Fig. 4). A number of potential scenarios can explain these observations. For one, the assays may have captured the enzymatic activity of *Nar* in lieu of *Nap*, if the former was expressed constitutively during aerobic growth. *Nap* may either not be expressed during aerobic growth (though some evidence points to the contrary; Sears et al. 1997) or its activity may be negligible compared to that of *Nar*. Alternatively, the *Nap* enzyme expressed by *P. denitrificans* may impart similar isotope effects on NO_3^- than *Nar*. Our results do not permit distinction among scenarios. We suspect that the assays were dominated by *Nar* activity, given the distinctive isotopic signature imparted on NO_3^- by *Nap* in other bacterial strains (see below). However, unlike other NO_3^- reductase groups, a high degree of functional and

genetic diversity is recognized among *Nap* enzymes (Sparacino-Watkins et al. 2014), which could be associated with different catalytic mechanisms among *Nap* enzymes, potentially manifest in NO_3^- isotope effects. Thus, the observations are inconclusive with respect to characterizing the isotope effects of *Nap* in *P. denitrificans*.

The periplasmic dissimilatory NO_3^- reductase *Nap* assayed from *R. sphaeroides* cell homogenates showed patterns of NO_3^- isotopic fractionation distinct from those of *P. denitrificans*. Assays were associated with a $\Delta\delta^{18}O{:}\Delta\delta^{15}N$ ratio of ~0.5, rather than ~1 observed for *Nar*. Moreover, the amplitudes of $^{15}\varepsilon_{Nap}$ of 39‰ is substantially more elevated than $^{15}\varepsilon_{Nar}$, whereas the corresponding $^{18}\varepsilon_{Nap}$ amplitude of 19‰ is lower than most observed values for $^{18}\varepsilon_{Nar}$. Assuming that enzymatic isotope effects are associated specifically with bond breakage and are not incurred from binding and unbinding of NO_3^- to the enzyme (Campbell 2001), the dissimilar enzymatic $\Delta\delta^{18}O{:}\Delta\delta^{15}N$ ratios portend of differences in $\varepsilon_{intrinsic}$, thus, in the respective transition states of *Nar* and *Nap*, indicating different kinetic mechanisms. This is surprising, given that (1) there are high structural and functional similarities between the catalytic sites of *Nap* and *Nar* and (2) analogous catalytic mechanisms are hypothesized for the two enzyme groups (Coelho and Romão 2015). Both *Nap* and *Nar* belong to the dimethylsulfoxide oxidase (DMSO) reductase family of molybdoenzymes, in which the Mo active site is coordinated by two molybdopterin guanidine dinucleotide (MGD) molecules, each providing two bidentate dithiolene ligands (Mo[MGD]$_2$; reviewed by Moreno-Vivian et al. 1999; Sparacino-Watkins et al. 2014). The coordination of *Nap*'s Mo atom is completed with a cysteine or selenium–cysteine ligand, whereas *Nar*'s is completed with an asparginine ligand. Both enzyme groups also possess an additional oxo/hydroxo/water ligand at the Mo atom. However, *Nap* is located in the bacterial periplasm, whereas *Nar* spans the inner bacterial membrane, with the NO_3^- reduction site oriented toward the cytoplasm. *Nap* receives electron from the ubiquinol pool via a membrane-anchored cytochrome *c* subunit that shuttles the electrons to a second, periplasmic subunit with cytochrome *c* group, followed by an iron sulfur cluster in the catalytic subunit that relays electrons to the Mo[MGD]$_2$ center. *Nar* receives electrons from the ubiquinol pool via a membrane bound biheme cytochrome *b* subunit that relays electrons to a soluble subunit consisting of three [4Fe-4S] clusters and one [3Fe-4S] cluster, then to the membrane-bound catalytic subunit via a [4Fe-4S] cluster to the Mo[MGD]$_2$ center (Fig. 6). The active site of *Nap* is reportedly specific to NO_3^-, save for observations of selenite reduction mediated by *Nap* (Gates et al. 2011), whereas *Nar*'s is relatively nonspecific and has been observed binding with other monocharged anions, such as fluoride, nitrite, formate, chlorate, and bromate (George et al. 1985; Jormakka et al. 2004).

The catalytic mechanisms of NO_3^- reduction by both *Nap* and *Nar* are currently though to involve direct oxygen atom transfer to the Mo atom (Coelho and Romão 2015).

However, ab initio computations on model complexes for *Nap* and *Nar* active sites suggest that NO_3^- reduction mediated by direct oxotransfer to the Mo atom should incur equivalent intrinsic N and O isotope effects for both enzyme types, on the order of ~33‰ (Guo et al. 2010). The discrepancy between computed vs. observed isotope effects for *Nap* suggests that the catalytic mechanism currently posited for *Nap* may be inaccurate and that NO_3^- reduction at the active site of *Nap* involves a different bonding environment than currently stipulated.

The enzymatic isotope effects measured in *R. sphaeroides* cell homogenates were nearly twofold greater than those observed in the growing cultures of *R. sphaeroides*, whereas the enzymatic $\Delta\delta^{18}O{:}\Delta\delta^{15}N$ ratios (0.50) were roughly comparable to those observed in cultures (0.57). Nevertheless, the isotope effects and $\Delta\delta^{18}O{:}\Delta\delta^{15}N$ ratios of the *R. sphaeroides* cultures are consistent with the range reported previously for cultures of *R. sphaeroides* (Granger et al. 2008), as well as similar to values observed in growing cultures of the autotrophic Epsilon-protoebacterium *Sufurimonas gotlandica* (Frey et al. 2014), which oxidizes sulfide for autotrophic carbon fixation while using NO_3^- as an electron donor via the periplasmic *Nap* NO_3^- reductase. The reduced isotope effects in *R. sphaeroides* cultures compared to in vitro could be hypothesized to indicate that ε_{Nap} is not fully expressed in the external medium due to incomplete equilibration of periplasmic and external NO_3^- pools. Yet, because *Nap* is a periplasmic enzyme (Fig. 1), the expression of ε_{Nap} in the external medium is ostensibly *not* modulated by active transport and cellular efflux. Porin channels in the outer membrane of Gram-negative bacteria allow the free diffusion of small hydrophilic molecules such as NO_3^- in and out of the periplasmic space (Galdiero et al. 2012; Fig. 1), presumably enabling complete homogenization between the periplasmic and external NO_3^- pools, which should permit full expression of enzymatic isotope effects of periplasmic enzymes. Moreover, reduced expression of the ε_{Nap} in vivo cannot be explained by diffusion limitation of $[NO_3^-]$ into the periplasm to the active site of *Nap*, because bacterial cells are too small and NO_3^- concentrations too high to result in a diffusive boundary layer, as argued previously (Pasciak and Gavis 1974; Granger et al. 2008; Kritee et al. 2012). In this respect, the similarity between isotope effects amplitudes in still vs. shaken cultures of *R. sphaeroides* observed here supports the notion that incomplete equilibration of periplasmic and external NO_3^- does not adequately explain the large offset from the enzymatic isotope effects measured in vitro. Nevertheless, Frey et al. (2014) reported a higher isotope effect for cultures of *S. gotlandica* that were shaken during growth vs. still cultures, a result they ascribed to putative intrabottle gradients in $[NO_3^-]$ caused by a higher degree of consumption by clumped cells at the bottom of the flasks in the still cultures, and consequent diffusion limitation of NO_3^- to the periplasmic enzyme site of the clumped cells. If

viable, this mechanism should have evidenced a progressive decrease in apparent isotope effects as NO_3^- was depleted. However, isotope effects in the still cultures of *S. gotlandica* were reduced from the onset of growth at highly elevated $[NO_3^-]$, and remained unchanged throughout growth, inconsistent with rationalizations involving diffusion limitation. Moreover, the in vitro enzymatic isotope effects observed here remain considerably higher than the values among shaken cultures of *S. gotlandica* ($^{15}\varepsilon = 19\text{‰}{-}28\text{‰}$), in which $^{15}\varepsilon_{Nap}$ should have been expressed fully, given complete equilibration of periplasmic and external NO_3^- pools ensured by shaking. Therefore, assuming that *R. sphaeroides* and *S. gotlantica* have analogous *Nap* enzymes, diffusion limitation does not to explain the relatively reduced isotope effects observed in cultures compared to in vitro. Rather, we posit that the reduced isotope effects of *Nap* in cultures compared to in vitro, as well as any differences in isotope effects in vivo, occur because the amplitude of *Nap* is variable in vivo, sensitive to catalytic rates as modulated by $[NO_3^-]$ in relation to cellular reductant concentrations, in analogy to *Nar* and *Nir*. The apparent decrease of $^{15}\varepsilon_{Nap}$ (and $^{18}\varepsilon_{Nap}$) with $[NO_3^-]$ in the growing cultures of *R. sphaeroides* (Fig. 4a) is consistent with this hypothesis. It follows that *Nap* assays fuelled by the in vivo reductant (ubiquinone) in lieu of viologen would reveal substrate sensitivity of ε_{Nap}. Admittedly, the seeming lack of sensitivity of ε_{Nap} to $[NO_3^-]$ in vitro in MeVi assays remains puzzling, as per observations with *Nar*, but could reflect the documented occurrence of kinetically distinct catalytic forms of the *Nap* enzyme (Frangioni et al. 2004).

While interesting from a biochemical perspective, the significance of NO_3^- isotope effects imparted by *Nap* for interpretation of environmental NO_3^- isotope distributions may be limited, as *Nap* is not apt to account bulk NO_3^- consumption in most environments. Unlike assimilatory and respiratory NO_3^- reductases that have conserved functionality (i.e., *Nar*, *eukNR*, and *Nas*, the bacterial assimilatory NO_3^- reductase), *Nap* is functionally diverse (reviewed by Sparacino-Watkins et al. 2014). *Nap* is generally cited to provide a means of disposing of excess electrons for maintenance of electrochemical balance during photoheterotrophic growth and during growth on reduced carbon substrates and is required for transition to anaerobeosis among heterotrophic denitrifiers (Sparacino-Watkins et al. 2014). In contrast to *Nar*, NO_3^- reduction by *Nap* does not directly generate a proton-motive force across the cytoplasmic membrane and, thus, is not a respiratory enzyme in-and-of-itself—although sulfide-oxidizing Epsilon-protoebacteria are capable of NO_3^- respiration via *Nap* (Kern and Simon 2009). In this respect, *Nap* has been postulated to influence the NO_3^- $\Delta\delta^{18}O{:}\Delta\delta^{15}N$ in systems where sulfide oxidation is coupled to NO_3^- reduction (Frey et al. 2014; Wenk et al. 2014a). *Nap* is further hypothesized to account for $\Delta\delta^{18}O{:}\Delta\delta^{15}N$ ratios < 1 prevalent in freshwater systems (Frey et al. 2014), although this

premise requires that *Nap* effectuate the majority of NO_3^- reduction therein. Given the universality of the characteristic $\Delta\delta^{18}O{:}\Delta\delta^{15}N$ ratio of $\sim$0.6 in groundwater aquifers and lakes (Kendall et al. 2007), its origin is explained more parsimoniously by the isotopic imprint of NO_3^- production, by nitrification and/or anammox, superimposed on that of respiratory denitrification by *Nar* (Granger and Wankel in review).

N and O isotope effects of eukaryotic assimilatory NO_3^- reductases, *eukNR*

The commercially prepared pure extracts of recombinant *eukNR* from *A. thalania* and *P. angusta* both yielded a $\Delta\delta^{18}O{:}\Delta\delta^{15}N$ ratio of $\sim$1, and $^{15}\varepsilon_{eukNR}$ of $\sim$27‰, consistent with previous observations in viologen-fuelled assays of purified *eukNR* from *Aspergillus* sp., and in cell homogenates of the diatom *T. weissflogii* (Karsh et al. 2012). The $\Delta\delta^{18}O{:}\Delta\delta^{15}N$ coupling and amplitude of N and O isotope effects observed among *eukNR* enzymes is also identical to values observed here in viologen-fuelled assays of *Nar*. This suggests similar catalytic mechanisms of *eukNR* and *Nar* enzymes groups. In this respect, *eukNR* enzymes cluster in a monophyletic group deriving from *Nar* enzymes (Stolz and Basu 2002). Both groups are mononuclear, hexadentate molybdoenzymes, although *eukNR* belongs to the sulfite oxidase family of molybdoenzymes with a single molybdopterin moiety involved in Mo coordination (Campbell 1999), whereas *Nar* belongs to the DMSO reductase family where coordination of the Mo active site involves two molybdopterin moeities. In this respect, the isotopic similarities between the two imply similar transition state structures of NO_3^- bound to Mo during catalysis.

Interestingly, the *eukNR* of *P. angusta* expressed recombinantly in yeast (YNar) constitutes a "simplified" eukaryotic NO_3^- reductase consisting of the amino-terminal fragment extending to the molybdopterin-binding site that forms the enzyme active site (Barbier et al. 2004). It does not include the cytochrome *b* reducing fragment or the heme-iron containing domain of *eukNR*, which are involved in electron transfer to the Mo active site. Viologen-fuelled NO_3^- reduction of this simplified NO_3^- reductase replicates isotope effects observed for whole *eukNR* enzymes, consistent with the understanding that viologen transfers electrons directly to the Mo active site. In this respect, the invariant $\Delta\delta^{18}O{:}\Delta\delta^{15}N$ ratio of $\sim$1 observed among *eukNR* enzymes and for *Nar* reinforces the notion that the isotopic coupling is intrinsic to the bond-breaking step at the catalytic site of both enzymes types, thus remaining invariant regardless of reductant type.

In analogy to *Nar*, the amplitude $^{15}\varepsilon_{eukNR}$ (and $^{18}\varepsilon_{eukNR}$) may be sensitive to catalytic rate, as modulated by the concentration of native reductants NADH and/or NADPH, in relation to $[NO_3^-]$. Such a sensitivity could explain why the enzymatic isotope effect, ε_{eukNR}, inferred from cultures of diatoms is on order of 22‰ (Karsh et al. 2014; Needoba et al.

2004), rather than 27‰ assumed based on viologen-fuelled *eukNR* assays. This premise needs to be tested directly.

Conclusions

Our results demonstrate that NO_3^- reduction by the respiratory NO_3^- reductase *Nar*, like *eukNR*, imparts an invariant $\Delta\delta^{18}O{:}\Delta\delta^{15}N$ ratio of ~ 1 on residual NO_3^-, reinforcing that this characteristic isotopic signature provides a robust benchmark to distinguish NO_3^- consumption by denitrification and assimilation from cooccurring N transformations. While tightly coupled to each other, the amplitude of the enzymatic isotope effect in vivo is likely variable, sensitive to internal $[NO_3^-]$ in relation to cellular reductant pools. This dynamic is consistent with a kinetic mechanism wherein the catalytic rate modulates overall expression of the intrinsic isotope effect at the enzyme level. In turn, *Nap* enzymatic isotope effects showed an invariant $\Delta\delta^{18}O{:}\Delta\delta^{15}N$ ratio of ~ 0.5, analogous to corresponding culture observations, yet relatively muted isotope effect amplitudes in vivo, which may result from a sensitivity of *Nap* isotope effects to cellular reductant pools and ambient $[NO_3^-]$. Together, these finding compel a reevaluation of the physiological mechanisms leading to variations in organism-level isotope effects during assimilatory and dissimilatory NO_3^- reduction.

References

Altabet, M. A. 2001. Nitrogen isotopic evidence for micronutrient control of fractional NO_3 utilization in the equatorial Pacific. Limnol. Oceanogr.. **46**: 368–380. doi:10.4319/lo.2001.46.2.0368

Amberger, A., and H. L. Schmidt. 1987. Natürliche isotopengehalte von nitrat als Indikatoren für dessen herkunft. Geochim. Cosmochim. Acta **51**: 2699–2705. doi:10.1016/0016-7037(87)90150-5

Anderson, L. J., D. J. Richardson, and J. N. Butt. 2001. Catalytic protein film voltammetry from a respiratory nitrate reductase provides evidence for complex electrochemical modulation of enzyme activity. Biochemistry **40**: 11294–11307. doi:10.1021/bi002706b

Aravena, R., and W. D. Robertson. 1998. Use of multiple isotope tracers to evaluate denitrification in ground water: Study of nitrate from a large-flux septic system plume. Ground Water **36**: 975–982. doi:10.1111/j.1745-6584.1998.tb02104.x

Barbier, G. G., R. C. Joshi, E. R. Campbell, and W. H. Campbell. 2004. Purification and biochemical characterization of simplified eukaryotic nitrate reductase expressed in *Pichia pastoris*. Protein Expr. Purif. **37**: 61–71. doi:10.1016/j.pep.2004.05.021

Barbier, G. G., and W. H. Campbell. 2005. Viscosity effects on eukaryotic nitrate reductase activity. J. Biol. Chem. **280**: 26049–26054. − doi:10.1074/jbc.M409694200

Barford, C. C., J. P. Montoya, M. A. Altabet, and R. Mitchell. 1999. Steady-state nitrogen isotope effects of N_2 and N_2O production in *Paracoccus denitrificans*. Appl. Environ. Microbiol. **65**: 989–994.

Bender, R. A., and B. Friedrich. 1990. Regulation of assimilatory nitrate reductase formation in *Klebsiella aerogenes* W70. J. Bacteriol. **172**: 7256–7259.

Berks, B. C., S. J. Ferguson, J. W. B. Moir, and D. J. Richardson. 1995. Enzymes and associated electron transport systems that catalyse the respiratory reduction of nitrogen oxides and oxyanions. Biochim. Biophys. Acta Bioenerget. **1232**: 97–173. doi:10.1016/0005-2728(95)00092-5

Böhlke, J. K., S. J. Mroczkowski, and T. B. Coplen. 2003. Oxygen isotopes in nitrate: New reference materials for O-18:O-17:O-16 measurements and observations on nitrate–water equilibration. Rapid Commun Mass Spectrom. **17**: 1835–1846. doi:10.1002/rcm.1123

Böttcher, J., O. Strebel, S. Voerkelius, and H. L. Schmidt. 1990. Using isotope fractionation of nitrate nitrogen and nitrate oxygen for evaluation of microbial denitrification in a sandy aquifer. J. Hydrol. **114**: 413–424. doi:10.1016/0022-1694(90)90068-9

Bourbonnais, A., M. A. Altabet, C. N. Charoenpong, J. Larkum, H. Hu, H. W. Bange, and L. Stramma. 2015. N-loss isotope effects in the Peru oxygen minimum zone studied using a mesoscale eddy as a natural tracer experiment. Glob. Biogeochem. Cycles **29**: 793–811. doi:10.1002/2014GB005001

Braman, R. S., and S. A. Hendrix. 1989. Nanogram nitrite and nitrate determination in environmental and biological materials by vanadium(Iii) reduction with chemiluminescence detection. Analyt. Chem. **61**: 2715–2718. doi:10.1021/ac00199a007

Brandes, J. A., A. H. Devol, T. Yoshinari, D. A. Jayakumar, and S. W. A. Naqvi. 1998. Isotopic composition of nitrate in the central Arabian Sea and eastern tropical North Pacific: A tracer for mixing and nitrogen cycles. Limnol. Oceanogr. **43**: 1680–1689. doi:10.4319/lo.1998.43.7.1680

Brandes, J. A., and A. H. Devol. 2002. A global marine-fixed nitrogen isotopic budget: Implications for holocene nitrogen cycling. Glob. Biogeochem. Cycles **16**:

Bryan, B. A., G. Shearer, J. L. Skeeters, and D. H. Kohl. 1983. Variable expression of the nitrogen isotope effect associated with denitrification of nitrite. J. Biol. Chem. **258**: 8613–8617.

Buchwald, C., A. E. Santoro, R. H. R. Stanley, and K. L. Casciotti. 2015. Nitrogen cycling in the secondary nitrite maximum of the eastern tropical North Pacific off Costa Rica. Glob. Biogeochem. Cycles **29**: 2061–2081. doi:10.1002/2015GB005187

Campbell, W. H. 1999. Nitrate reductase structure, function and regulation: Bridging the gap between biochemistry

and physiology. Annu. Rev. Plant Physiol. Plant Mol. Biol. **50**: 277–303. doi:10.1146/annurev.arplant.50.1.277

Campbell, W. H. 2001. Structure and function of eukaryotic NAD(P)H: Nitrate reductase. Cell. Mol. Life Sci. **58**: 194–204. doi:10.1007/PL00000847

Carlisle, E., C. Yarnes, M. D. Toney, and A. J. Bloom. 2014. Nitrate reductase 15N discrimination in *Arabidopsis thaliana*, *Zea mays*, *Aspergillus niger*, *Pichea angusta*, and *Escherichia coli*. Front. Plant Sci. **5**: 317. doi: 10.3389/fpls.2014.00317

Casciotti, K. L. 2016. Nitrogen and oxygen isotopic studies of the marine nitrogen cycle, p. 379–407. *In* C. A. Carlson and S. J. Giovannoni [eds.], Annual review of marine science. V. **8**: 379–407. doi: 10.1146/annurev-marine-010213-135052

Casciotti, K. L., D. M. Sigman, M. G. Hastings, J. K. Bohlke, and A. Hilkert. 2002. Measurement of the oxygen isotopic composition of nitrate in seawater and freshwater using the denitrifier method. Analyt. Chem. **74**: 4905–4912. doi:10.1021/ac020113w

Casciotti, K. L., and M. R. McIlvin. 2007. Isotopic analyses of nitrate and nitrite from reference mixtures and application to Eastern Tropical North Pacific waters. Mar. Chem. **107**: 184–201. doi:10.1016/j.marchem.2007.06.021

Casciotti, K. L., C. Buchwald, and M. McIlvin. 2013. Implications of nitrate and nitrite isotopic measurements for the mechanisms of nitrogen cycling in the Peru oxygen deficient zone. Deep-Sea Res. I **80**: 78–93. doi:10.1016/j.dsr.2013.05.017

Coelho, C., and M. J. Romão. 2015. Structural and mechanistic insights on nitrate reductases. Protein Sci. **24**: 1901–1911. doi:10.1002/pro.2801

Cook, P. F. 1991. Kinetic and regulatory mechanisms of enzymes from isotope effects, p. 203–230. *In* P. F. Cook [ed.], Enzyme mechanism from isotope effects. CRC Press, Boca Raton, FL.

Dabundo, R. 2014. Nitrogen isotopes in the measurement of N_2-fixation and the estimation for denitrification in the global ocean. University of Connecticut, Storrs, CT.

Deutsch, C., D. M. Sigman, R. C. Thunell, A. N. Meckler, and G. H. Haug. 2004. Isotopic constraints on glacial/interglacial changes in the oceanic nitrogen budget. Glob. Biogeochem. Cycles **18**. doi: 10.1029/2003GB002189

DeVries, T., C. Deutsch, P. A. Rafter, and F. Primeau. 2013. Marine denitrification rates determined from a global 3-D inverse model. Biogeosciences **10**: 2481–2496. doi: 10.5194/bg-10-2481-2013

DiFiore, P. J., D. M. Sigman, T. W. Trull, M. J. Lourey, K. L. Karsh, G. Cane, and R. Ho. 2006. Nitrogen isotope constraints on subantarctic biogeochemistry. J. Geophys. Res. Oceans **111**: C08016. doi: 10.1029/2005JC003216

Elliott, S. J., K. R. Hoke, K. Heffron, M. Palak, R. A. Rothery, J. H. Weiner, and F. A. Armstrong. 2004. Voltammetric studies of the catalytic mechanism of the respiratory

nitrate reductase from *Escherichia coli*: How nitrate reduction and inhibition depend on the oxidation state of the active site. Biochemistry **43**: 799–807. doi:10.1021/bi035869j

Eugster, O., and N. Gruber. 2012. A probabilistic estimate of global marine N-fixation and denitrification. Glob. Biogeochem. Cycles **26**: GB4013. doi: 10.1029/2012GB004300

Frangioni, B., P. Arnoux, M. Sabaty, D. Pignol, P. Bertrand, B. Guigliarelli, and C. Leger. 2004. In *Rhodobacter sphaeroides* respiratory nitrate reductase, the kinetics of substrate binding favors intramolecular electron transfer. J. Am. Chem. Soc. **126**: 1328–1329. doi:10.1021/ja0384072

Frey, C., S. Hietanen, K. Jürgens, M. Labrenz, and M. Voss. 2014. N and O isotope fractionation in nitrate during chemolithoautotrophic denitrification by *Sulfurimonas gotlandica*. Environ. Sci. Technol. **48**: 13229–13237. doi: 10.1021/es503456g

Galdiero, S., A. Falanga, M. Cantisani, R. Tarallo, M. E. Della Pepa, V. D'Oriano, and M. Galdiero. 2012. Microbe–host interactions: Structure and role of Gram-negative bacterial porins. Curr. Protein Pept. Sci. **13**: 843–854. v. pii: CPPS-EPUB-20121210-11. doi:10.2174/138920312804871120

Garside, C. 1982. A chemiluminescent technique for the determination of nanomolar concentration of nitrate and nitrite in seawater. Mar. Chem. **11**: 159–167. doi:10.1016/0304-4203(82)90039-1

Gates, A. J., C. S. Butler, D. J. Richardson, and J. N. Butt. 2011. Electrocatalytic reduction of nitrate and selenate by NapAB. Biochem. Soc. Trans. **39**: 236–242. doi:10.1042/BST0390236

Gaye, B., B. Nagel, K. Dähnke, T. Rixen, and K. C. Emeis. 2013. Evidence of parallel denitrification and nitrite oxidation in the ODZ of the Arabian Sea from paired stable isotopes of nitrate and nitrite. Glob. Biogeochem. Cycles **27**: 1059–1071. doi:10.1002/2011GB004115

George, G. N., R. Bray, F. Morpeth, and D. Boxer. 1985. Complexes with halide and other anions of the molybdenum centre of nitrate reductase from *Escherichia coli*. Biochem. J. **227**: 925–931. doi:10.1042/bj2270925

Gonfiantini, R., W. Stichler, and K. Rosanski. 1995. Standards and intercomparison materials distributed by the IAEA for stable isotope measurements. International Atomic Energy Agency, Vienna.

Granger, J., D. M. Sigman, J. A. Needoba, and P. J. Harrison. 2004. Coupled nitrogen and oxygen isotope fractionation of nitrate during assimilation by cultures of marine phytoplankton. Limnol. Oceanogr. **49**: 1763–1773. doi: 10.4319/lo.2004.49.5.1763

Granger, J., D. M. Sigman, M. G. Prokopenko, M. F. Lehmann, and P. D. Tortell. 2006. A method for nitrite removal in nitrate N and O isotope analyses. Limnol. Oceanogr. Methods **4**: 205–212. doi:10.4319/lom.2006.4.205

Granger, J., D. M. Sigman, M. F. Lehmann, and P. D. Tortell. 2008. Nitrogen and oxygen isotope fractionation during dissimilatory nitrate reduction by denitrifying bacteria. Limnol. Oceanogr. **53**: 2533–2545. doi:10.4319/lo.2008.53.6.2533

Granger, J., and D. M. Sigman. 2009. Removal of nitrite with sulfamic acid for nitrate N and O isotope analysis with the denitrifier method. Rapid Commun. Mass Spectrom. **23**: 3753–3762. doi:10.1002/rcm.4307

Granger, J., D. M. Sigman, M. M. Rohde, M. T. Maldonado, and P. D. Tortell. 2010. N and O isotope effects during nitrate assimilation by unicellular prokaryotic and eukaryotic plankton cultures. Geochim. Cosmochim. Acta **74**: 1030–1040. doi:10.1016/j.gca.2009.10.044

Gruber, N., and J. N. Galloway. 2008. An Earth-system perspective of the global nitrogen cycle. Nature **451**: 293–296. doi:10.1038/nature06592

Guillard, R. R. L. 1975. Culture of phytoplankton for feeding marine invertebrates, p. 22–60. *In* W. L. Smith and M. H. Chanley [eds.], Culture of marine invertebrate animals. Plenum Press, New York.

Guo, W., J. Granger, and D. M. Sigman. 2010. Nitrate isotope fractionations during biological nitrate reduction: Insights from first principles theoretical modeling. *In* AGU 2010 fall meeting. San Francisco, CA.

Jepson, B. J., and others. 2004. Tuning a nitrate reductase for function: The first spectropotentiometric characterization of a bacterial assimilatory nitrate reductase reveals novel redox properties. J Biol Chem. **279**: 32212–32218. doi:10.1074/jbc.M402669200

Jormakka, M., D. Richardson, B. Byrne, and S. Iwata. 2004. Architecture of NarGH reveals a structural classification of Mo-bisMGD enzymes. Structure **12**: 95–104. doi:10.1016/j.str.2003.11.020

Karsh, K. L., T. W. Trull, A. J. Lourey, and D. M. Sigman. 2003. Relationship of nitrogen isotope fractionation to phytoplankton size and iron availability during the Southern Ocean Iron RElease Experiment (SOIREE). Limnol. Oceanogr. **48**: 1058–1068. doi:10.4319/lo.2003.48.3.1058

Karsh, K. L., J. Granger, K. Kritee, and D. M. Sigman. 2012. Eukaryotic assimilatory nitrate reductase fractionates N and O isotopes with a ratio near unity. Environ. Sci. Technol. **46**: 5727–5735. doi:10.1021/es204593q

Karsh, K. L., Trull, T. W. D. M. Sigman, T P. A., and J. Granger. 2014. The contributions of nitrate uptake and efflux to isotope fractionation during algal nitrate assimilation. Geochim. Cosmochim. Acta. **132**: 391–412. doi:10.1016/j.gca.2013.09.030

Kendall, C., E. M. Elliott, and S. D. Wankel. 2007. Tracing anthropogenic inputs of nitrogen to ecosystems, p. 375–449. Wiley-Blackwell, Malden, MA, USA.

Kern, M., and J. Simon. 2009. Electron transport chains and bioenergetics of respiratory nitrogen metabolism in *Wolinella succinogenes* and other Epsilonproteobacteria. Biochim. Biophys. Acta Bioenerget. **1787**: 646–656. doi:10.1016/j.bbabio.2008.12.010

Knöller, K., C. Vogt, M. Haupt, S. Feisthauer, and H. H. Richnow. 2011. Experimental investigation of nitrogen and oxygen isotope fractionation in nitrate and nitrite during denitrification. Biogeochemistry **103**: 371–384. doi:10.1007/s10533-010-9483-9

Korner, H., and W. G. Zumft. 1989. Expression of denitrification enzymes in response to the dissolved oxygen levels and respiratory substrate in continuous culture of *Pseudomonas stutzeri*. Appl. Environ. Microbiol. **55**: 1670–1676.

Kritee, K., D. M. Sigman, J. Granger, B. B. Ward, A. Jayakumar, and C. Deutsch. 2012. Reduced isotope fractionation by denitrification under conditions relevant to the ocean. Geochim. Cosmochim. Acta. **92**: 243–259. doi:10.1016/j.gca.2012.05.020

Mariotti, A., J. C. Germon, P. Hubert, P. Kaiser, R. Letolle, A. Tardieux, and P. Tardieux. 1981. Experimental determination of nitrogen kinetic isotope fractionation: Some principles; illustration for the denitrification and nitrification processes. Plant Soil **62**: 413–430. doi:10.1007/BF02374138

Montoya, J. P., and J. J. McCarthy. 1995. Isotopic fractionation during nitrate uptake by marine phytoplankton grown in continuous culture. J. Plankton Res. **17**: 439–464. doi:10.1093/plankt/17.3.439

Moreno-Vivian, C., P. Cabello, M. Martinez-Luque, R. Blasco, and F. Castillo. 1999. Prokaryotic nitrate reduction: Molecular properties and functional distinction among bacterial nitrate reductases. J. Bacteriol. **181**: 6573–6584.

Needoba, J. A., N. A. Waser, P. J. Harrison, and S. E. Calvert. 2003. Nitrogen isotope fractionation in 12 species of marine phytoplankton during growth on nitrate. Mar. Ecol. Prog. Ser. **255**: 81–91. doi:10.3354/meps255081

Needoba, J. A., D. M. Sigman, and P. J. Harrison. 2004. The mechanism of isotope fractionation during algal nitrate assimilation as illuminated by the N-15/N-14 of intracellular nitrate. J. Phycol. **40**: 517–522. doi:10.1111/j.1529-8817.2004.03172.x

O'Leary, M. H. 1980. Determination of heavy-atom isotope effects on enzyme-catalyzed reactions. Methods Enzymol. **64**: 881–888.

Pasciak, W. J., and J. Gavis. 1974. Transport limitation of nutrient uptake in phytoplankton. Limnol. Oceanogr. **19**: 881–898. doi:10.4319/lo.1974.19.6.0881

Peltzer, E. T. 2007. MATLAB shell-scripts for linear regression analysis, l. Least-Squares-Cubic, http://www.mbari.org/index-of-downloadable-files/.

Sears, H. J., S. Spiro, and D. J. Richardson. 1997. Effect of carbon substrate and aeration on nitrate reduction and expression of the periplasmic and membrane-bound nitrate reductases in carbon-limited continuous cultures of *Paracoccus denitrificans* Pd1222. Microbiology **143**: 3767–3774. doi:10.1099/00221287-143-12-3767

Shearer, G., J. D. Schneider, and D. H. Kohl. 1991. Separating the efflux and influx components of net nitrate uptake by Synechococcus-R2 under steady-state conditions. J. General Microbiol. **137**: 1179–1184.

Sigman, D. M., M. A. Altabet, R. Francois, D. C. McCorkle, and G. Fischer. 1999. The d^{15}N of nitrate in the Southern Ocean: Consumption of nitrate in surface waters. Glob. Biogeochem. Cycles **13**: 1149–1166. doi:10.1029/1999GB900038

Sigman, D. M., K. L. Casciotti, M. Andreani, C. Barford, M. Galanter, and J. K. Bohlke. 2001. A bacterial method for the nitrogen isotopic analysis of nitrate in seawater and freshwater. Analyt. Chem. **73**: 4145–4153. doi:10.1021/ac010088e

Sigman, D. M., J. Granger, P. J. DiFiore, M. M. Lehmann, R. Ho, G. Cane, and A. van Geen. 2005. Coupled nitrogen and oxygen isotope measurements of nitrate along the eastern North Pacific margin. Glob. Biogeochem. Cycles **19**:

Skipper, L., W. H. Campbell, J. A. Mertens, and D. J. Lowe. 2001. Pre-steady-state kinetic analysis of recombinant *Arabidopsis* NADP: Nitrate reductase-rate-limiting processes in catalysis. J. Biol. Chem. **276**: 26995–27002. − doi:10.1074/jbc.M100356200

Sokal, R. R., and F. J. Rohlf. 1995. Biometry: The principles and practice of statistics in biological research, 3rd ed. Freeman, W. H., New York.

Sparacino-Watkins, C., J. F. Stolz, and P. Basu. 2014. Nitrate and periplasmic nitrate reductases. Chem. Soc. Rev. **43**: 676–706. doi:10.1039/C3CS60249D

Stolz, J. F., and P. Basu. 2002. Evolution of nitrate reductase: Molecular and structural variations on a common function. Chembiochem **3**: 198–206. doi:10.1002/1439-7633(20020301)3:2/3<198::AID-CBIC198>3.0.CO;2-C

Voss, M., J. W. Dippner, and J. P. Montoya. 2001. Nitrogen isotope patterns in the oxygen-deficient waters of the eastern tropical North Pacific Ocean. Deep-Sea Res. I **48**: 1905–1921. doi:10.1016/S0967-0637(00)00110-2

Wada, E., and A. Hattori. 1978. Nitrogen isotope effects in the assimilation of inorganic nitrogenous compounds. Geomicrobiol. J. **1**: 85–101. doi:10.1080/01490457809377725

Waser, N. A., K. D. Yin, Z. M. Yu, K. Tada, P. J. Harrison, D. H. Turpin, and S. E. Calvert. 1998. Nitrogen isotope fractionation during nitrate, ammonium and urea uptake by marine diatoms and coccolithophores under various conditions of N availability. Mar. Ecol. Prog. Ser. **169**: 29–41. doi:10.3354/meps169029

Waser, N. A., Z. M. Yu, K. D. Yin, B. Nielsen, P. J. Harrison, D. H. Turpin, and S. E. Calvert. 1999. Nitrogen isotopic fractionation during a simulated diatom spring bloom: Importance of N-starvation in controlling fractionation. Mar. Ecol. Prog. Ser. **179**: 291–296. doi:10.3354/meps179291

Weaver, P. F., J. D. Wall, and H. Gest. 1975. Characterization of *Rhodopseudomonas capsulata*. Arch. Microbiol. **105**: 207–216. doi:10.1007/BF00447139

Wellman, R. P., F. D. Cook, and H. R. Krouse. 1968. Nitrogen-15: Microbiological alteration of abundance. Science **161**: 269–270. doi:10.1126/science.161.3838.269

Wenk, C. B., J. Zopfi, J. Blees, M. Veronesi, H. Niemann, and M. F. Lehmann. 2014a. Community N and O isotope fractionation by sulfide-dependent denitrification and anammox in a stratified lacustrine water column. Geochim. Cosmochim. Acta **125**: 551–563. doi:10.1016/j.gca.2013.10.034

Wenk, C. B., J. Zopfi, W. S. Gardner, M. J. McCarthy, H. Niemann, M. Veronesi, and M. F. Lehmann. 2014b. Partitioning between benthic and pelagic nitrate reduction in the Lake Lugano south basin. Limnol. Oceanogr. **59**: 1421–1433. doi:10.4319/lo.2014.59.4.1421

Wu, J. P., S. E. Calvert, and C. S. Wong. 1997. Nitrogen isotope variations in the subarctic northeast Pacific: Relationships to nitrate utilization and trophic structure. Deep-Sea Res. I **44**: 287–314. doi:10.1016/S0967-0637(96)00099-4

Wunderlich, A., R. Meckenstock, and F. Einsiedl. 2012. Effect of different carbon substrates on nitrate stable isotope fractionation during microbial denitrification. Environ. Sci. Technol. **46**: 4861–4868. doi:10.1021/es204075b

Wunderlich, A., R. U. Meckenstock, and F. Einsiedl. 2013. A mixture of nitrite-oxidizing and denitrifying microorganisms affects the δ18O of dissolved nitrate during anaerobic microbial denitrification depending on the δ18O of ambient water. Geochim. Cosmochim. Acta **119**: 31–45. doi:10.1016/j.gca.2013.05.028

Acknowledgments

Conflict of Interest

None declared.